



Calhoun: The NPS Institutional Archive

Theses and Dissertations

Thesis Collection

1955

The effects of scanning on the detection of targets.

Perszyk, Joseph S.

Monterey, California. Naval Postgraduate School

<http://hdl.handle.net/10945/24701>



Calhoun is a project of the Dudley Knox Library at NPS, furthering the precepts and goals of open government and government transparency. All information contained herein has been approved for release by the NPS Public Affairs Officer.

Dudley Knox Library / Naval Postgraduate School
411 Dyer Road / 1 University Circle
Monterey, California USA 93943

<http://www.nps.edu/library>

THE EFFECTS OF SCANNING ON
THE DETECTION OF TARGETS

JOSEPH S. PERSZYK, JR.

Library
U. S. Naval Postgraduate School
Monterey, California

THE EFFECTS OF SCANNING
ON
THE DETECTION OF TARGETS

* * * * *

Joseph S. Perszyk, Jr.

THE EFFECTS OF SCANNING
ON THE DETECTION OF TARGETS

by

Joseph Stanley Perszyk, Jr.
Lieutenant, United States Navy

Submitted in partial fulfillment
of the requirements
for the degree of
MASTER OF SCIENCE
IN
ENGINEERING ELECTRONICS

United States Naval Postgraduate School
Monterey, California

1 9 5 5

Thesis

P 362

This work is accepted as fulfilling
the thesis requirements for the degree of

MASTER OF SCIENCE
IN
ENGINEERING ELECTRONICS

from the
United States Naval Postgraduate School

PREFACE

When a radar is employed to search for a target it is necessary to move the antenna beam about to scan an area. The introduction of this motion will have an effect on the detection capability of the radar. It is the aim of this paper to examine various scanning methods and parameters to determine their effect on the probability of detection and to provide a basis for a decision as to the most desirable scanning process to use.

The work on this paper was accomplished during the third term industrial experience tour at the Hughes Aircraft Company, Culver City, California.

The writer wishes to thank Dr. H. V. Hance and Mr. G. W. Zeoli of the Hughes Aircraft Company for their assistance, encouragement and cooperation in the preparation of this paper.

TABLE OF CONTENTS

Item	Title	Page
Chapter I	Introduction	1
Chapter II	Scanning Methods	8
Chapter III	Variation of Parameters	13
Chapter IV	Cumulative Probability of Detection . .	26
Chapter V	Illustrative Example	40
Chapter VI	Discussion of Results	46
Bibliography	48
Appendix I	Derivation of Expression for Probability of Detection	49
Appendix II	Description of Approximate Method for Obtaining Probability of Detection	54

LIST OF ILLUSTRATIONS

Figure	Page
1. Probability of Detection as a Function of \bar{x} , \bar{n} , and a	7
2. One Bar Single Look Probability Comparison of Scanning Methods	10
3. Two Bar Single Cycle Probability Comparison of Scanning Methods	11
4. Optimized Two Bar Single Cycle Probability Comparison of Scanning Methods	12
5. Variation of Probability of Detection With n	15
6. Effect of Varying Half Power Beam Width for Various Normalized Elevations	17
7. Linear Scan One Line Probability of Detection as a Function of Normalized Elevation	18
8. Palmer Scan One Line Probability of Detection as a Function of Normalized Elevation	19
9. One Line Linear Scan Probability of Detection for an Antenna with 4° Beam Width as a Function of θ_{HP} and Normalized Elevation	20
10. One Line Palmer Scan Probability of Detection for an Antenna with 4° Beam Width as a Function of θ_{HP} and Normalized Elevation	21
11. Palmer Scan, Variation of P_D with Squint Angle for Various Normalized Elevations	23
12. Palmer Scan, Variation of P_D with Normalized Elevation for Various Squint Angles	24
13. Linear Scan One Bar P_D as a Function of R/R_0 for Various Normalized Elevations	27
14. Linear Scan One Bar P_D as a Function of Normalized Elevations for Various R/R_0	28

Figure	Page
15. Linear Scan, One Cycle Two Bar P_D as a Function of Normalized Elevation for Various R/R_0	29
16. Linear Scan, One Bar Cumulative Probability of Detection as a Function of R/R_0 for Various Normalized Elevations	30
17. Linear Scan, One Bar Single Look P_D for $\bar{n} = 15$ and $\bar{n} = 25$ as a Function of Normalized Elevation	32
18. Linear Scan, One Bar Axial Cumulative Probability of Detection as a Function of R/R_0 for a Normalized Closing Rate of 0.01 for $\bar{n} = 15$	33
19. Linear Scan, One Bar Axial P_D vs R/R_0 for a Normalized Closing Rate of 0.05 for $\bar{n} = 15$	34
20. Linear Scan, One Bar Axial P_D vs R/R_0 for a Normalized Closing Rate of 0.10 for $\bar{n} = 15$	35
21. Normalized Range at Which $P_D = 0.85$ as a Function of n	37
22. Normalized Range at Which $P_D = 0.85$ as a Function of Half Power Beam Width	38
23. Single Cycle Probability of Detection as a Function of Normalized Elevation for Various Scanning Systems	44
24. Cumulative Probability of Detection at an Elevation of 0° as a Function of R/R_0 for Various Scanning Systems	45

TABLE OF SYMBOLS, ABBREVIATIONS AND TERMS

(Listed in the order of their use in the text)

R_{\max}	- Maximum Range At Which A Target Can Be Detected
S_{\min}	- Minimum Signal Power Required For Detection
P	- Peak Transmitted Power
G	- Antenna Gain
σ	- Scattering Cross Section of the Target
F	- Factor Which Allows For Plumbing Losses In Both Transmission And Reception
G_o	- Antenna Gain On The Axis Of The Beam
θ	- Angle Between Beam Axis And Target Position
θ_o	- Angle At Which The Antenna Gain Is 0.5
θ_{HP}	- Half Power Beam Width Of Antenna
P_D	- Single Look Probability Of Detection
Y_b	- Decision Bias
n	- Number of Pulses Integrated
$I()$	- Incomplete Gamma Function
\bar{x}	- Average Signal To Noise Ratio At Beam Center
a_i	- Signal To Noise Ratio Decrease Factor Due To Antenna Gain For i^{th} Pulse
W	- Integration Corridor Width
PRF	- Pulse Repetition Frequency
v	- Antenna Azimuth Scan Velocity
f	- Circular Scan Frequency of a Palmer Scan
ρ	- Squint Angle

Linear Scan	- Scanning Method in Which the Antenna is Moved in Azimuth at a Velocity v with all Pulses Occurring on the Scan Axis
Two Line Scan	- Antenna Motion is Such that Pulses Occur when the Beam Center is Offset Above and Below the Scan Axis by an Angle
Three Line Scan	- Motion is Such That Pulses Occur Successively at $+\rho$, 0 and $-\rho$.
Palmer Scan	- The Antenna is Rotated in a Circle of Radius r at Scan Frequency f and Simultaneously Moved in Azimuth with a Velocity v .
y_o/θ_{HP}	- Normalized Elevation Angle
\bar{n}	- Average Number of Pulses Integrated
R_o	- Range at Which the Signal to Noise Ratio is Unity
R	- Actual Range
R/R_o	- Normalized Range
$\Delta R/R_o$	- Normalized Closing Rate
x_i	- Actual Signal To Noise Ratio
B	- Receiver Band Width
NF	- Receiver Noise Figure
T	- Absolute Temperature
k	- Boltzman's Constant
a	- Antenna Gain Factor

CHAPTER I

INTRODUCTION

The earliest attempts to determine the detection capability of a radar did so on the basis of the maximum range at which a target could be detected for a given set of conditions.⁹ One form of this expression is:

$$R_{\max}^4 = \frac{PG^2 \lambda^2 \sigma F}{(4\pi)^3 S_{\min}}$$

where

R_{\max} - Maximum range of detection

S_{\min} - The minimum power required for detection

P - Peak transmitted power

G - Antenna gain

σ - Scattering cross section of the target

F - Factor which allows for plumbing losses
in both transmission and reception

Due to the random nature of receiver noise, which may have any value, the factor S_{\min} is a statistical quantity. Also, σ is not constant, but may vary radically for small changes in target aspect angle.

This variation in σ has been found to be statistical in nature for closing aircraft targets. These factors lead to the treatment of the detection problem on a statistical basis utilizing the probability of detection as a criterion.^{2,4,5,10}

Previous studies of the probability of detection have assumed the antenna gain to be constant between the half power points and zero

elsewhere, with correction factors used to approximate the effect of scanning.^{2,4,5,10} It is the purpose of this paper to extend these studies to the actual case where the antenna gain is not constant but is a function of the angular distance between the target and the beam center position with particular emphasis on the case of a narrow beam antenna whose gain in the target direction can be described as:

$$G = G_0 e^{-(\theta/\theta_0)^2}$$

where

G_0 - Antenna gain on the axis of the beam

θ - Angle between beam axis and target position

θ_0 - The angle for which $e^{-(\frac{\theta_{HP}}{2\theta_0})^2} = 0.5$

θ_{HP} - Antenna half power beam width

To this end the equation for the probability of detection, P_D , has been modified to include the effect of the antenna gain varying from pulse to pulse and a simplifying approximation for obtaining P_D has been developed.

The probability of detecting a slowly scintillating target on a single scan by a pulsed radar using a square law detector and a biased perfect integrator is: (See Appendix I for derivation and explanation of terms)

$$1. \quad P_D = 1 - I\left[\frac{Y_b}{\sqrt{n-1}}, n-2\right] + I\left[\frac{Y_b}{\left(1 + \frac{1}{\bar{x} \sum_{i=1}^n a_i}\right) \sqrt{n-1}}, n-2\right] \left(1 + \frac{1}{\bar{x} \sum_{i=1}^n a_i}\right)^{n-1} \times e^{-\frac{Y_b}{1 + \bar{x} \sum_{i=1}^n a_i}}$$

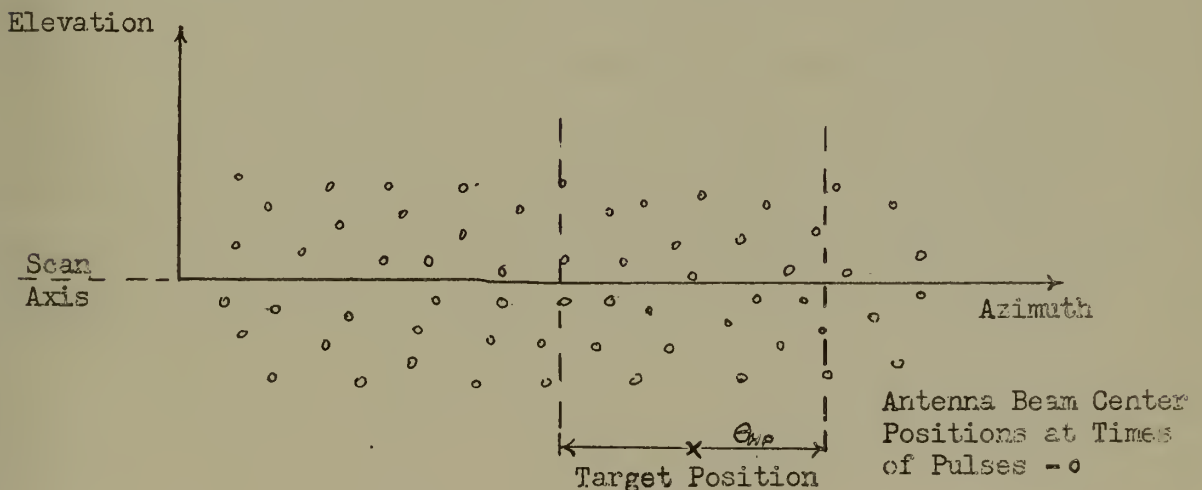
In the region of interest this can be approximated by

$$2. \quad P_D \approx \left(1 + \frac{1}{\bar{x}} \sum_{i=1}^n a_i\right)^{n-1} e^{-\frac{1}{1 + \bar{x}} \sum_{i=1}^n a_i}$$

with very little error.

In applying equation 2. to a particular scanning case it is necessary to determine the value of $\sum_{i=1}^n a_i$ for various assumed positions of the target. To do this one must first decide how many pulses to count. Some sort of a dividing line must be drawn, for if all of the pulses transmitted by the radar were counted P_D would have a ridiculously low value.

In a type B or PPI presentation each of the pulses transmitted at a given azimuth will produce a range sweep at the same azimuth position on the CRT face. Extending this thought to pulses transmitted over a range of azimuth positions it can be seen that the elevation of the antenna at the time of the pulse will not affect the presentation and hence the integration process at the face of the tube. In considering a given scan situation such as that shown below the summation will largely be determined by those pulses occurring while the antenna



beam center is below the scan axis while those above will contribute little.

Those pulses occurring while the beam center is above the axis will, however, produce range sweeps and must be considered in determining the decision bias. The proper procedure is therefore to consider all of the pulses which occur in a vertical corridor centered at the assumed target position.

As yet unresolved is the question as to how wide the above mentioned corridor should be. In a type B or PPI presentation the operator may be thought of as integrating over small areas of the presentation. This may be considered to be spatial integration performed by the eye-brain combination as differing from the electronic integration on the face of the CRT. No exact information as to the size of the area considered by the operator has been found. However, working on the premise that a strong target will present a blip whose width is slightly greater than the half power beam width of the antenna and that an operator would expect a weak target to present a slightly narrower blip, it was decided that a corridor width equal to the half power beam width would be a good starting point. To determine the effect of this assumption on the probability of detection for various corridor widths was determined. It was found that the curve of P_D vs corridor width, W , reached a maximum value for a corridor width equal to the half power beam width and was essentially flat, to within 1%, over a region $W = 0.9$ to 1.2 .

In most radar systems there is no synchronization between the scan cycle and the pulse repetition frequency. This leads to an uncertainty as to the azimuth position of the first pulse, since the first pulse will not necessarily occur at the start of the azimuth sweep but may occur anywhere within a distance in azimuth determined by the PRF, the azimuth scan velocity, v , and the method of scan employed. The distance between the start of the sweep and the initial pulse is referred to in this paper as starting phase. In the Palmer Scan there is an additional factor which affects the elevation position as well as the azimuth position, which is the angular distance between the initial pulse of the scan on the circular pattern and the zero reference angle of the circle. Once the circular scanning motion has started, the pulses will occur at successive positions on the circle as determined by the PRF and scanning frequency. The position of the initial pulse, however, may be anywhere on the circle. The angle between the initial pulse and the zero reference angle for the circle is termed initial phase.

The value of P_D for any assumed target position will depend upon the assumed starting phase and, where applicable, initial phase. To obtain a meaningful value of P_D for the target position it is necessary to determine the mean value of P_D averaged over all values of starting and initial phase.

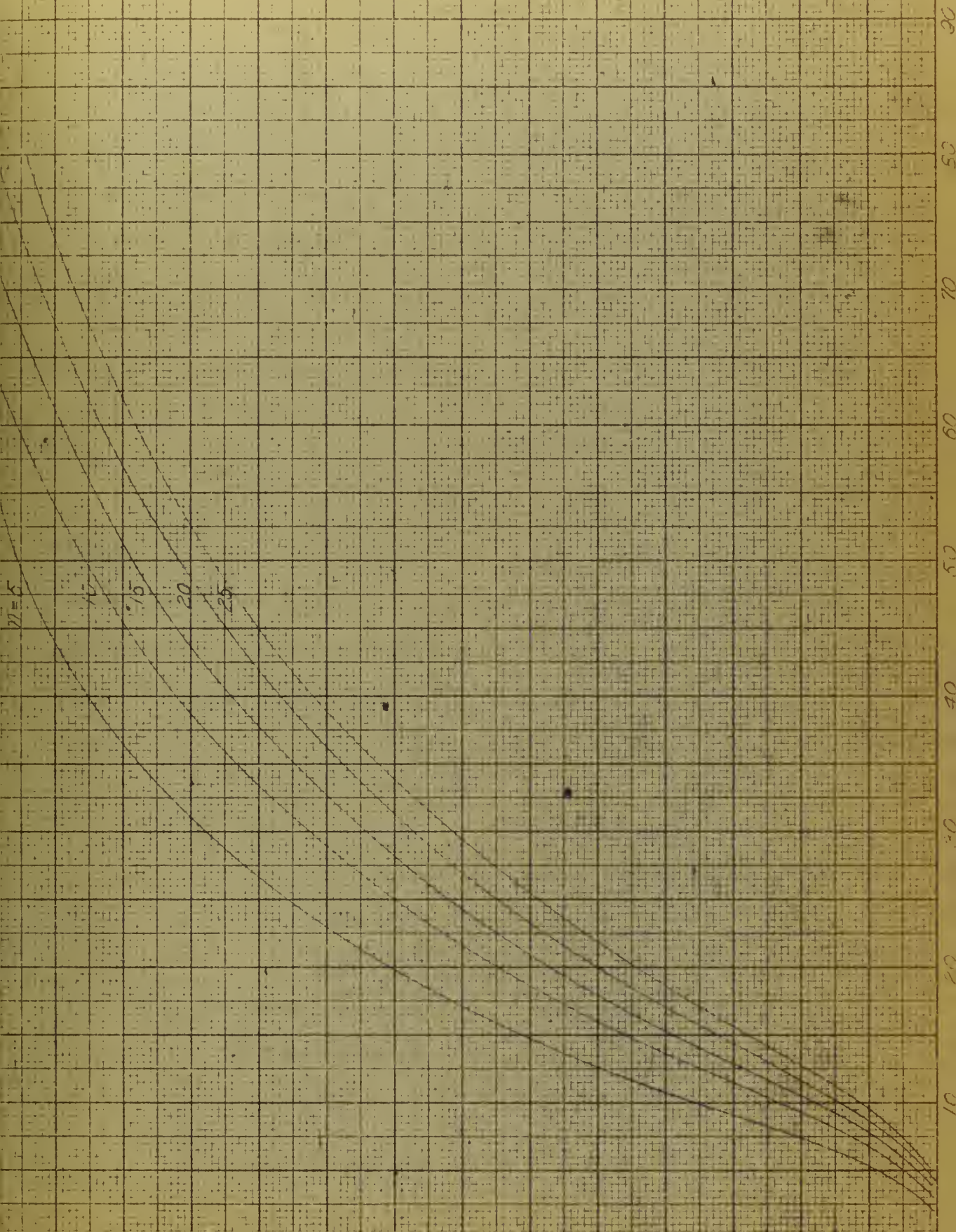
The amount of calculation required to determine this mean value of P_D lead to the development of an approximation for $\sum_{i=1}^N a_i$ for an antenna whose gain is $G = G_0 e^{-\left(\frac{\theta}{\theta_0}\right)^2}$ (see appendix II) for use in

obtaining P_D . The small error introduced was considered a small price to pay for the comparative ease with which the computations could be made.

The curves used herein are all based on the use of this approximation, and an ideal operator. Sample calculations over the range of interest show the results obtained with this simplified expression are accurate to within 15%.

Probability of Detection as a
Function of \bar{x} , \bar{n} , and a

FIG. 1



CHAPTER II

SCANNING METHODS

The function of an airborne fire control radar when employed in the search mode is to detect a target which may be anywhere within a given area. To accomplish this, with the narrow beam of this type radar, it is necessary to scan the area in both elevation and azimuth. This is done in azimuth by moving the beam along a horizontal line, called the scan axis, frequently with some sort of vertical perturbation to increase the elevation coverage. The area is scanned in elevation by shifting the scan axis to a new elevation and repeating the azimuth sweep. Each separate elevation is referred to as a bar.

The first step in the investigation of scanning methods is to determine the elevation coverage for a single bar. Figure 2 depicts the difference in elevation coverage for a given radar employing the four different scanning methods described below:

Linear Scan - The antenna is scanned in azimuth at a velocity v with all pulses occurring on the scan axis.

Two Line Scan - The antenna is scanned so that pulses occur when the beam center is offset above and below the scan axis by an angle ρ , called the squint angle.

Three Line Scan - The motion is such that the pulses occur successively at $+\rho$, 0 and $-\rho$.

Palmer Scan - The antenna beam is rotated in a circle of radius ρ at scan frequency f and simultaneously moved in azimuth with a velocity v .

In determining the increased elevation coverage due to the use of more than one bar it is necessary to use the principle of cumulative probability which is simply one minus the product of the probabilities of the operator not detecting the target on each of the bars.

$$P_D = 1 - \prod_{i=1}^m [1 - P_D(i)]$$

where $P_D(i)$ is the probability of detecting the target on the i^{th} bar and m equals the number of bars in one complete scan.

The exact separation of the bars is a matter of extreme importance as too great a separation will result in a "hole" in the elevation coverage, while too close spacing will be wasteful of the equipment's capabilities, as shown in Figure 3. Figure 4 shows the elevation coverage of the four scanning methods described above with the bar separation of each adjusted to give a reasonably constant value for P_D in the region between bars.

One Bar Single Lock Probability
Comparison of Scanning Methods

FIG. 2

1 - LINEAR SCAN

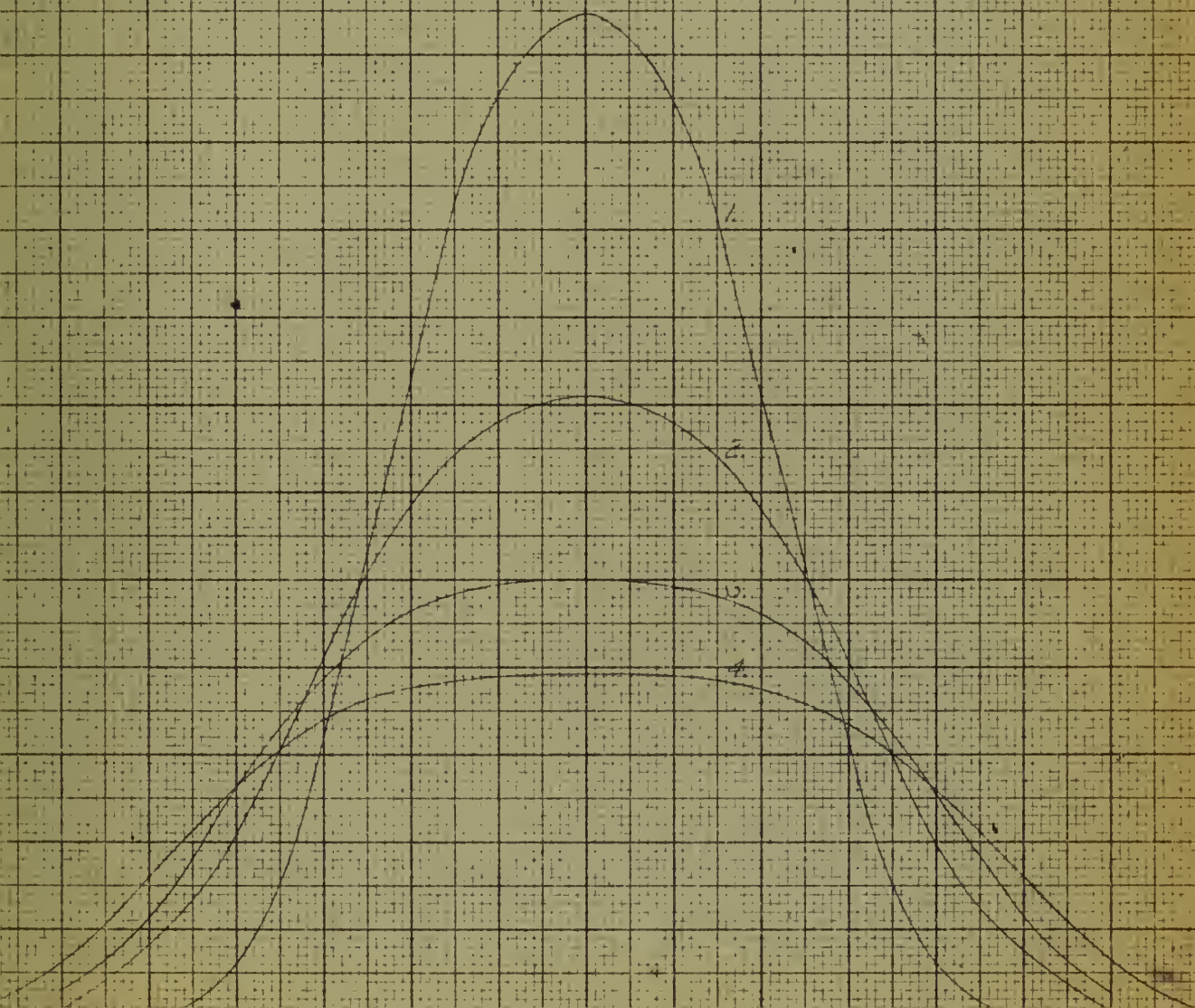
2 - TWO-LINE SCAN - $P = 0.5$ GND

3 - FALLOUT SCAN - $P = 0.5$ GND

4 - THREE-LINE SCAN - $P = 0.5$ GND

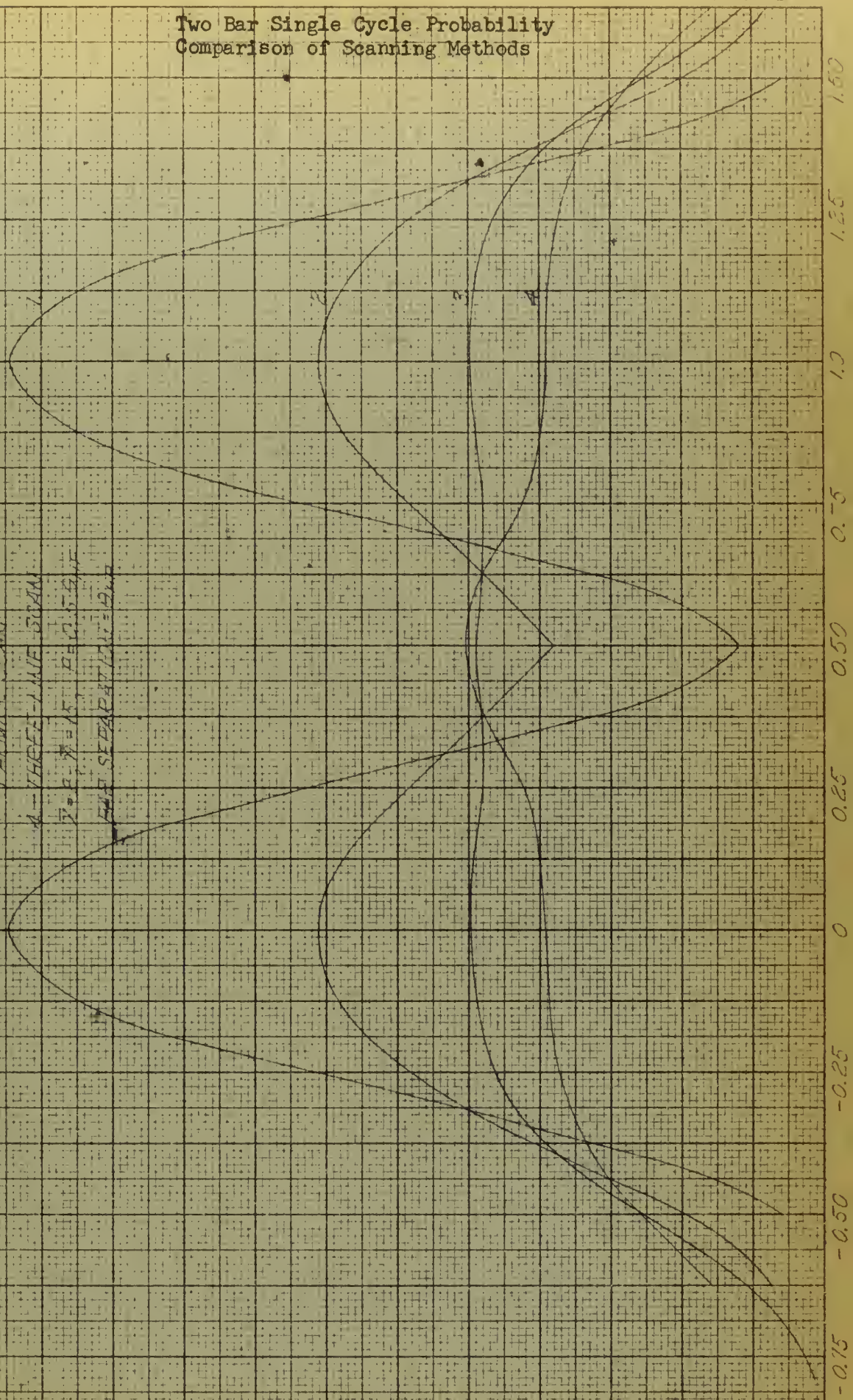
$P = 0.5$, $N = 15$

SCAN AXIS



Two Bar Single Cycle Probability Comparison of Scanning Methods

FIG. 5

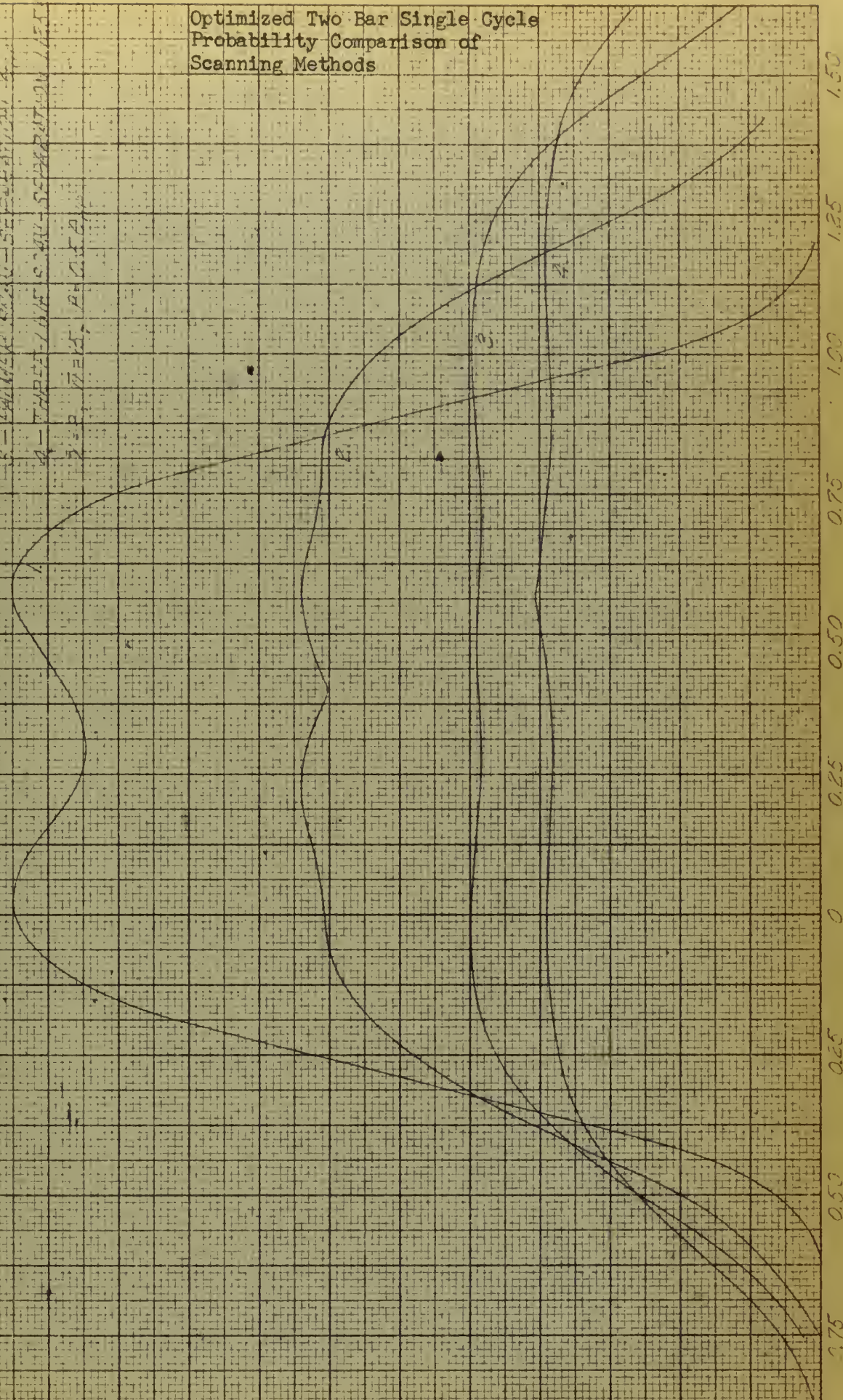


Optimized Two Bar Single Cycle Probability Comparison of Scanning Methods

FIG. 4

- 1- LINEAR SCAN-SEPARATION 1.6 mm
- 2- TWO-BAR SCAN-SEPARATION 0.8 mm
- 3- FASTER SCAN-SEPARATION 0.8 mm
- 4- THREE-BAR SCAN-SEPARATION 1.6 mm

2-3-4, $\bar{P}=15$, $P=2.5 \bar{P}$



CHAPTER III

VARIATION OF PARAMETERS

For a single bar of any given scanning method the designer has at his disposal the following factors which determine the probability of detection and elevation coverage for the type scan employed:

v - Azimuth Scan Velocity

PRF- Pulse Repetition Frequency

θ_{HP} - Half Power Beam Width

ρ - Squint Angle

f - The Scanning Frequency (Palmer Scan)

This section will consider individually the effects of the quantities listed above to demonstrate their effect on the single look P_D for a one bar scan.

Effects of Varying PRF and Azimuth Scan Velocity

The average number of pulses within the corridor, \bar{n} , is determined by

$$\bar{n} = \theta_{HP} \times \frac{PRF}{v}$$

θ_{HP} = Half Power Beam Width

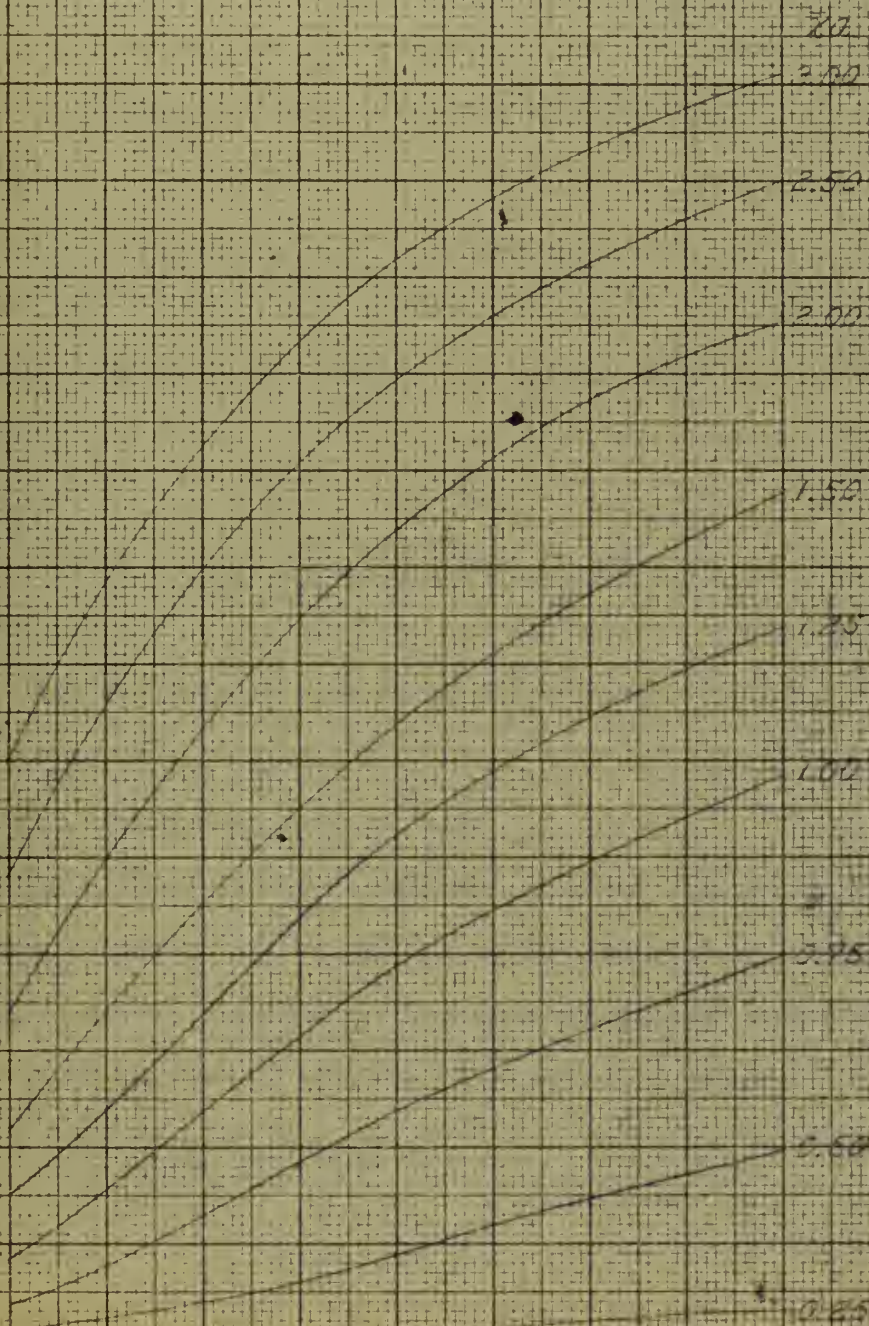
PRF = Pulse Repetition Frequency in cps

v - Azimuth Scan Velocity in degrees per second

Since \bar{n} is the only factor affected by PRF and v , Figure 5, which shows the effect of varying \bar{n} for various values of \bar{x}_a , represents the variation of P_D for any type scan.

Variation of Probability
of Detection with n

7/9-5



Effects of Changing Antenna Half Power Beam Width

Changing antenna half power beam width, Θ_{HP} , while holding all other parameters constant will result in the following:

- 1) The average number of pulses \bar{n} will change directly with Θ_{HP} .
- 2) The antenna gain will change inversely as the square of the change, hence the average signal to noise ratio, \bar{x} , will vary inversely as the fourth power of the change in beam width.

To investigate these effects a reference system was selected with parameters such that $\bar{n} = 15$ and $\bar{x} = 2$. The beam width was then changed to various multiples of its original value and the single look probability of detection determined from the new values of \bar{n} and \bar{x} . This is equivalent to changing the antenna size of a given radar system and determining its effect on the probability of detection for a given target.

Figures 6 and 7 show the result of changing Θ_{HP} for a linear scan. Figure 8 gives similar information for a Palmer Scan.

Figures 9 and 10 show the effect of decreasing the beam width of an antenna whose original half power beam width is 4° used in a Linear Scan and Palmer Scan respectively.

The primary effect illustrated in these figures is the improvement in single look single bar P_D due to the increase in signal-to-noise ratio obtained by decreasing Θ_{HP} . The more significant effect of changing half power beam width, that on the cumulative probability of detection, will be discussed in Chapter IV.

Effect of Varying Half Power Beam Width for Various Normalized Elevations

F/F₀ = 0

$\frac{S_0}{H}$ HP

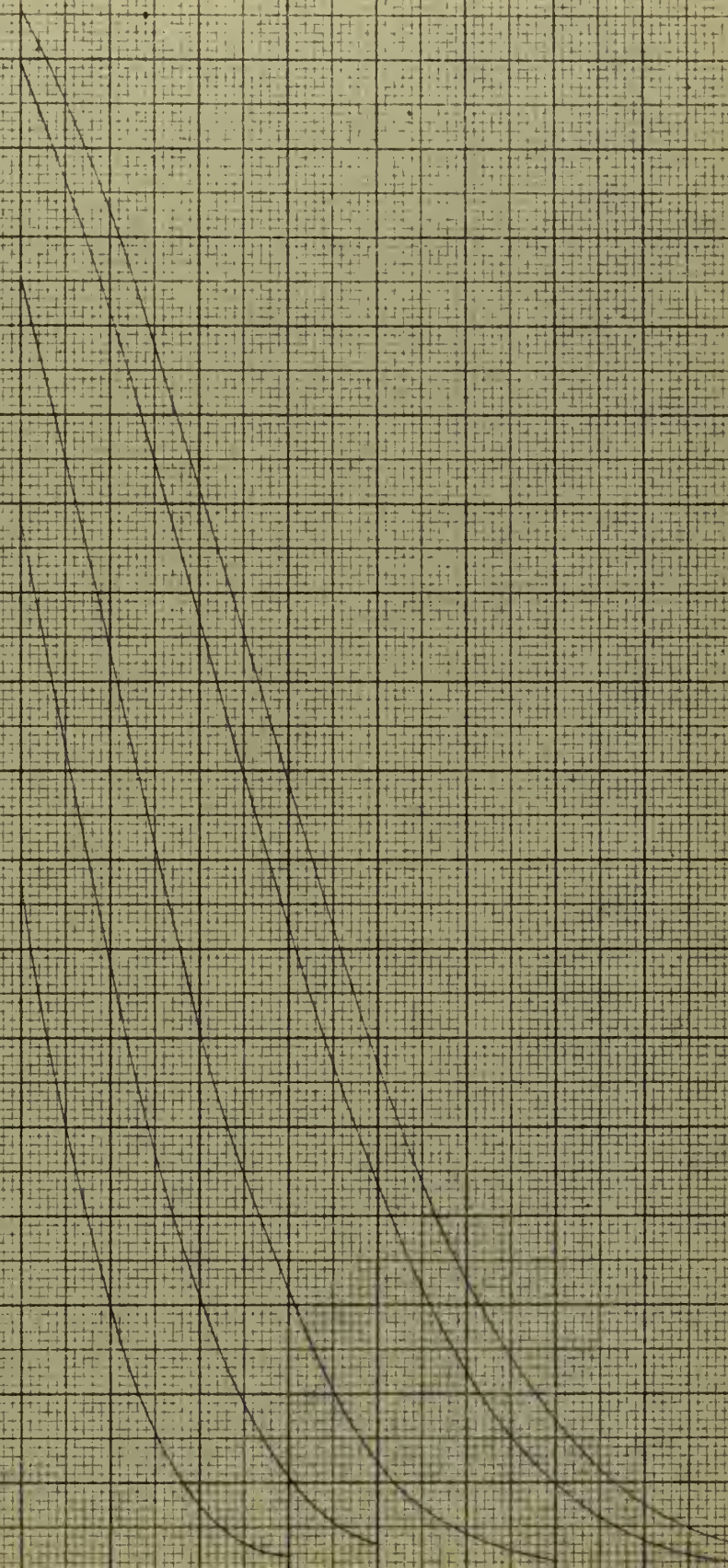
0

0.2

0.4

0.6

0.8

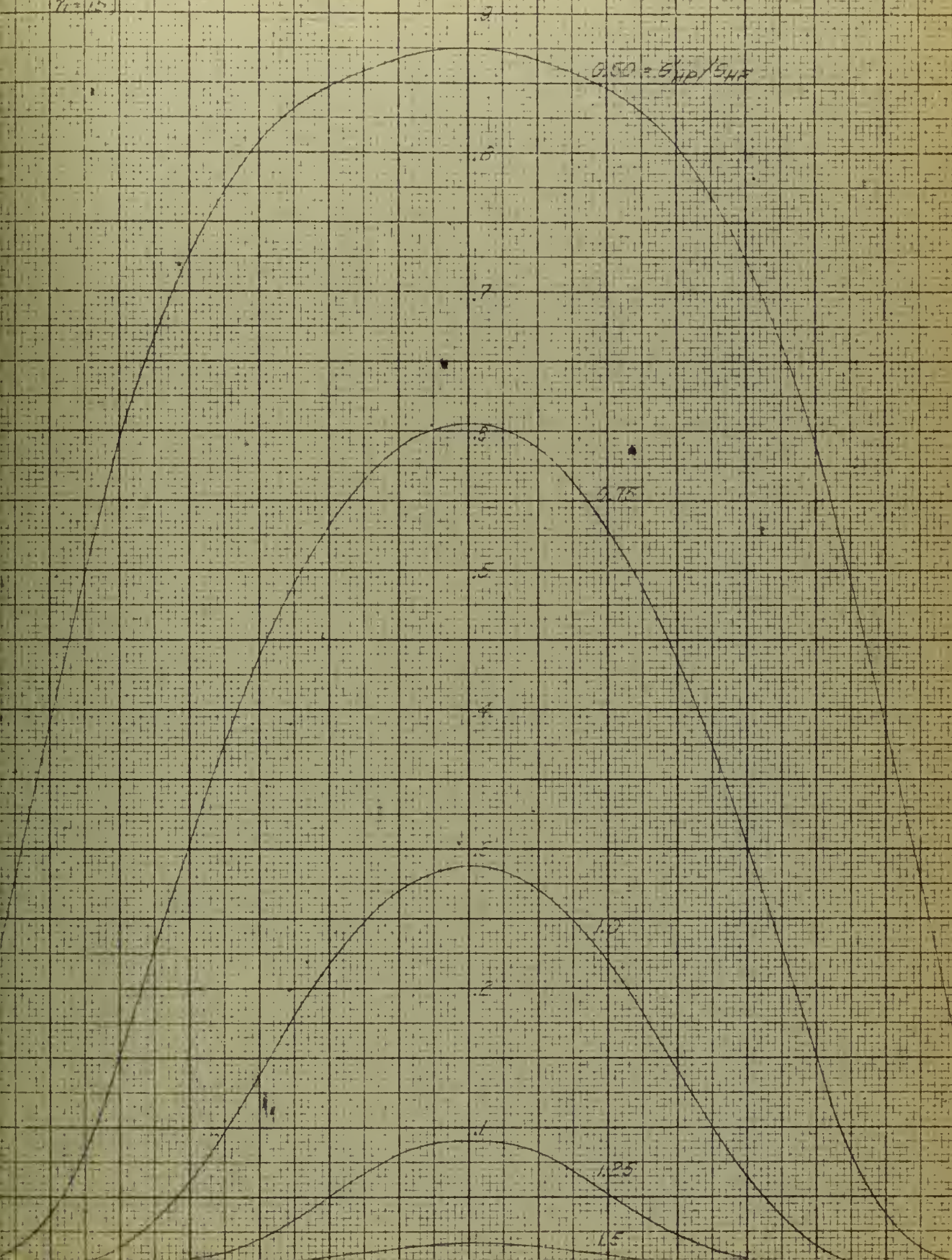


Linear Scan One Line Probability of Detection as a Function of Normalized Elevation

FIG. 7

$\bar{X} = 2.1$
 $\bar{Y} = 1.5$ $\frac{S_{HP}}{S_{HF}} = 1$

P_D



Palmer Scan One Line Probability of Detection as a Function of Normalized Elevation

7-19-58

$$P = 0.5 \theta_{HP}$$

$$Z = 2$$

$$\bar{P} = 15$$

$$\left. \begin{array}{l} P_{HP} / \theta_{HP} = 1 \end{array} \right\}$$

P_D

.75

.60

.55

.40

.35

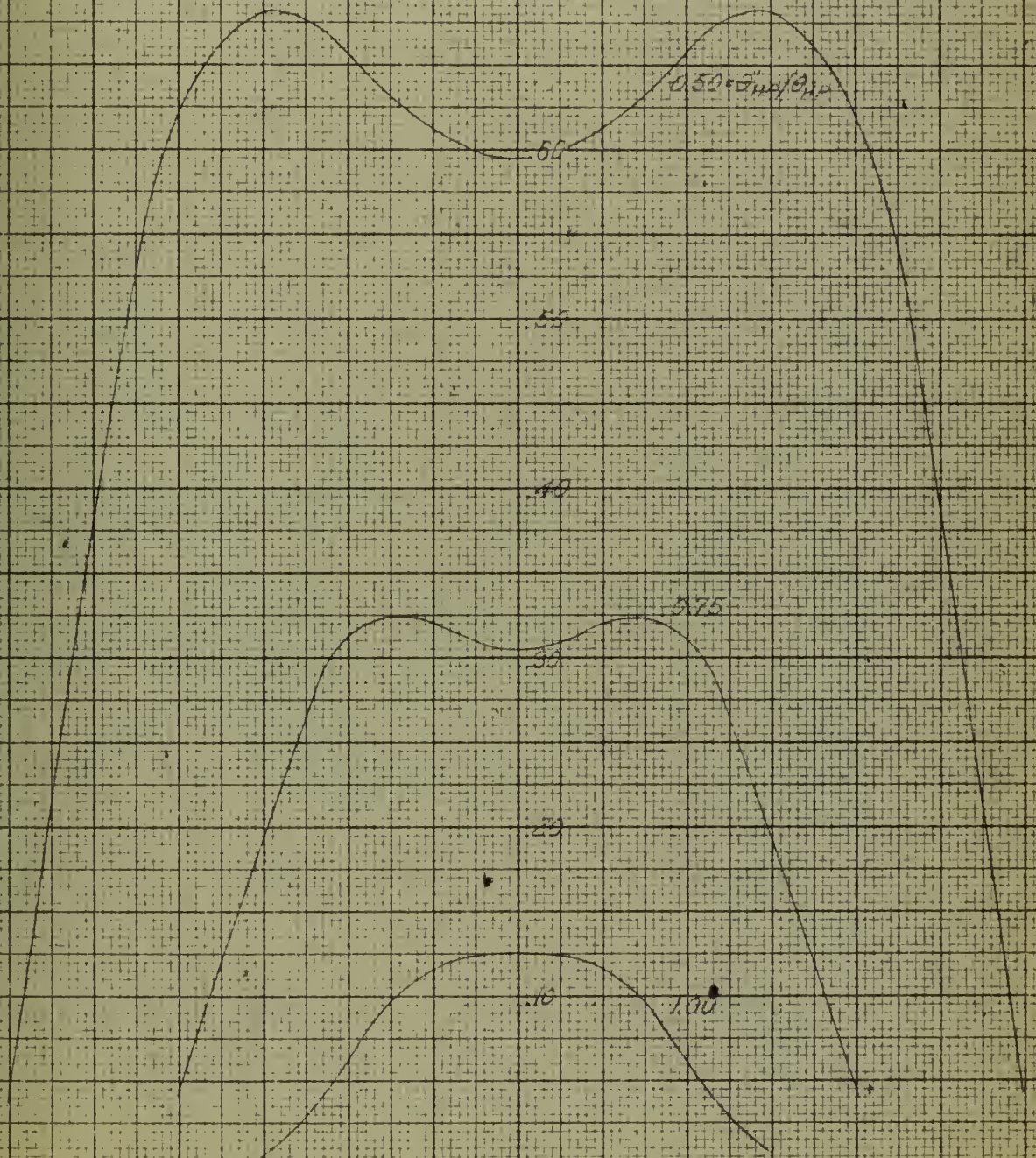
.20

.10

$$0.50 \theta_{HP} / \theta_{HP}$$

0.75

1.00



One Line Linear Scan Probability of De-
tection for an Antenna with 4° Beam Width
as a Function of OHP and Normalized Elevation

FIG. 3

$$\bar{P} = 2$$

$$\bar{P} = 15$$

$$\bar{P} = 20$$

$$G_{HP} = 1^\circ$$

$$10$$

$$9$$

$$8$$

$$7$$

$$6$$

$$5$$

$$4$$

$$3$$

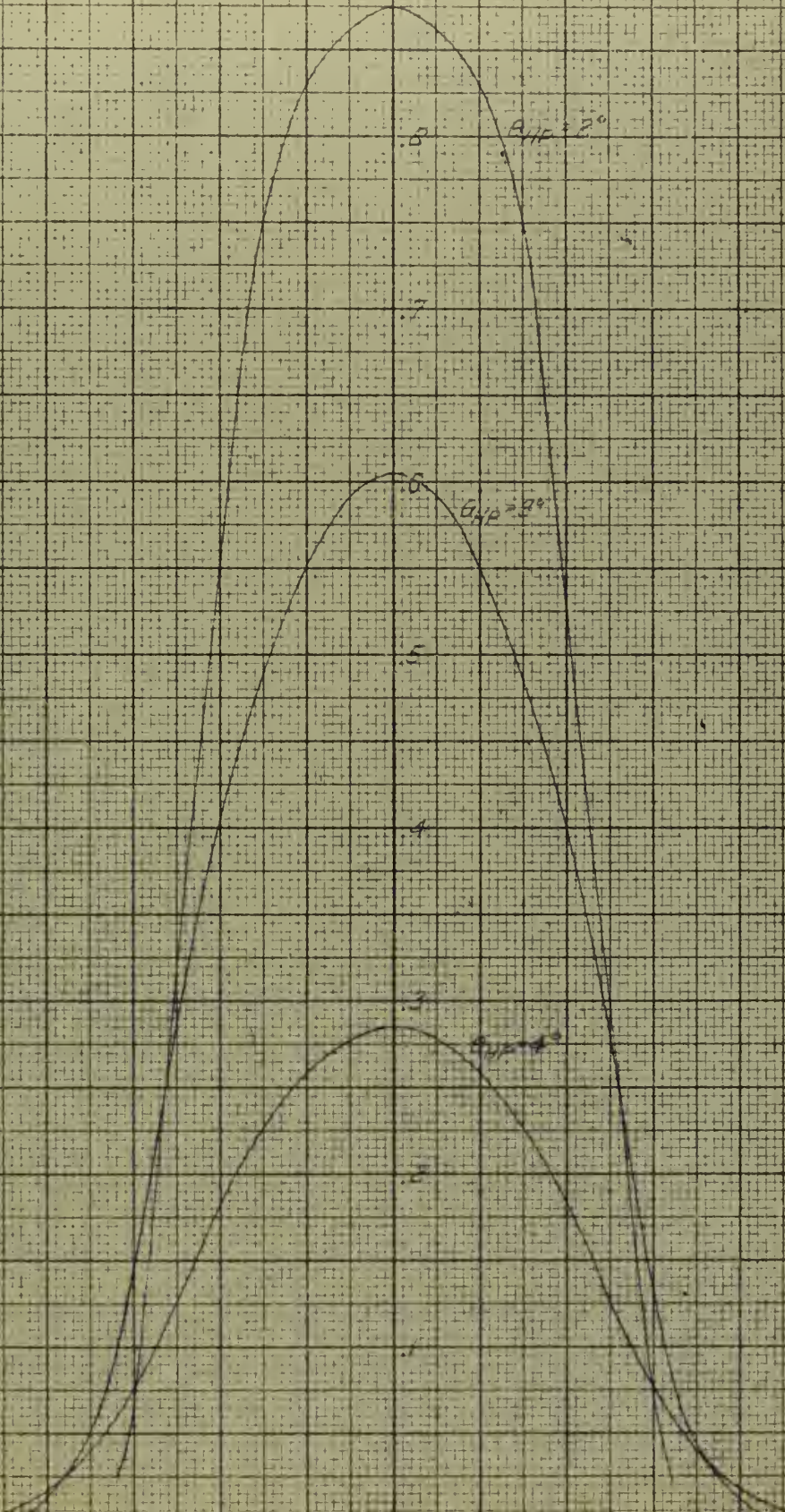
$$2$$

$$1$$

$$G_{HP} = 2^\circ$$

$$G_{HP} = 3^\circ$$

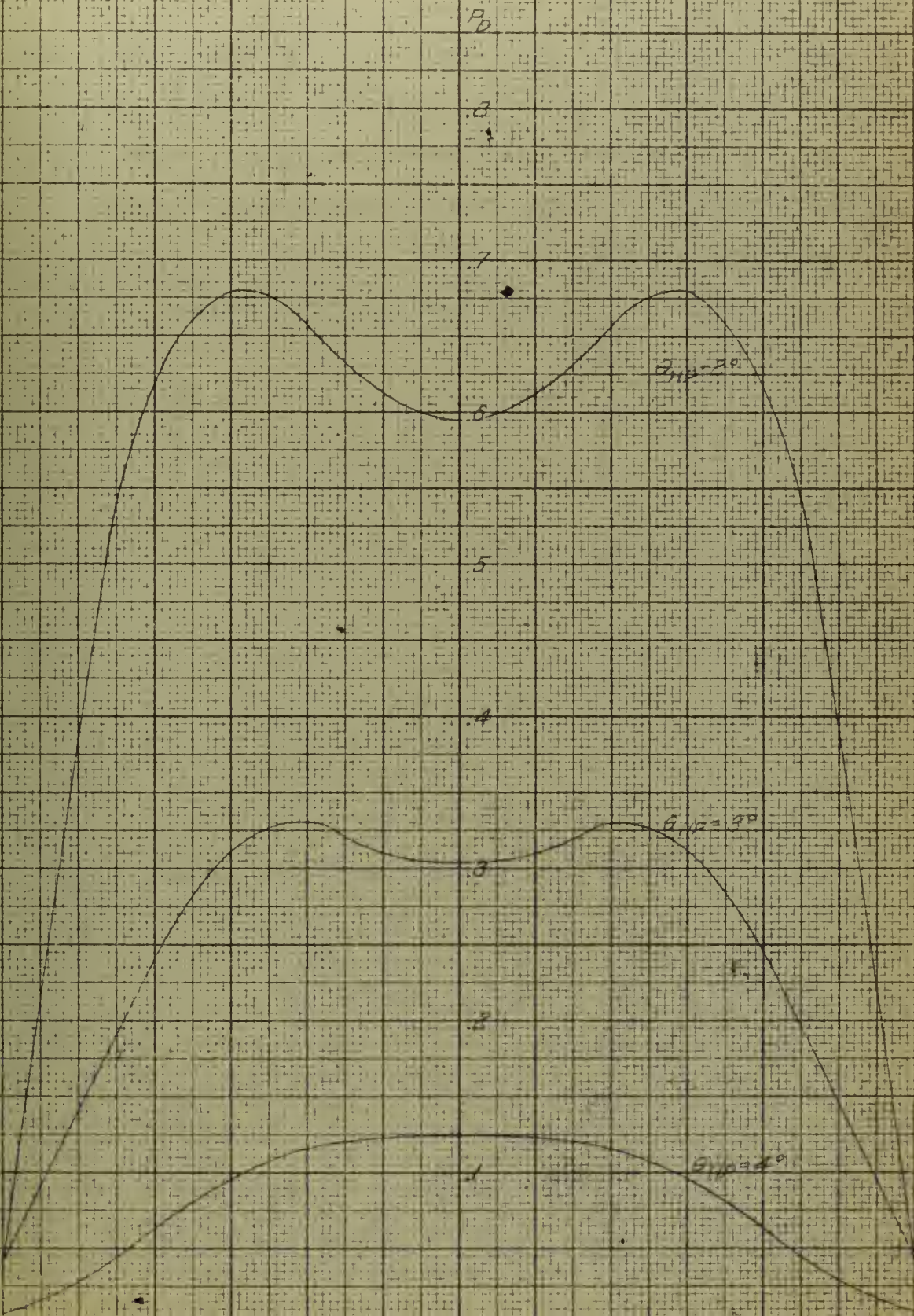
$$G_{HP} = 4^\circ$$



One Line Palmer Scan Probability of De-
 tection for an Antenna with 4° Beam Width
 as a Function of O_{HP} and Normalized Elevation

FIG. 10

$R=2$
 $N=15, \theta_{HP}=4^\circ$
 $P=5^\circ$



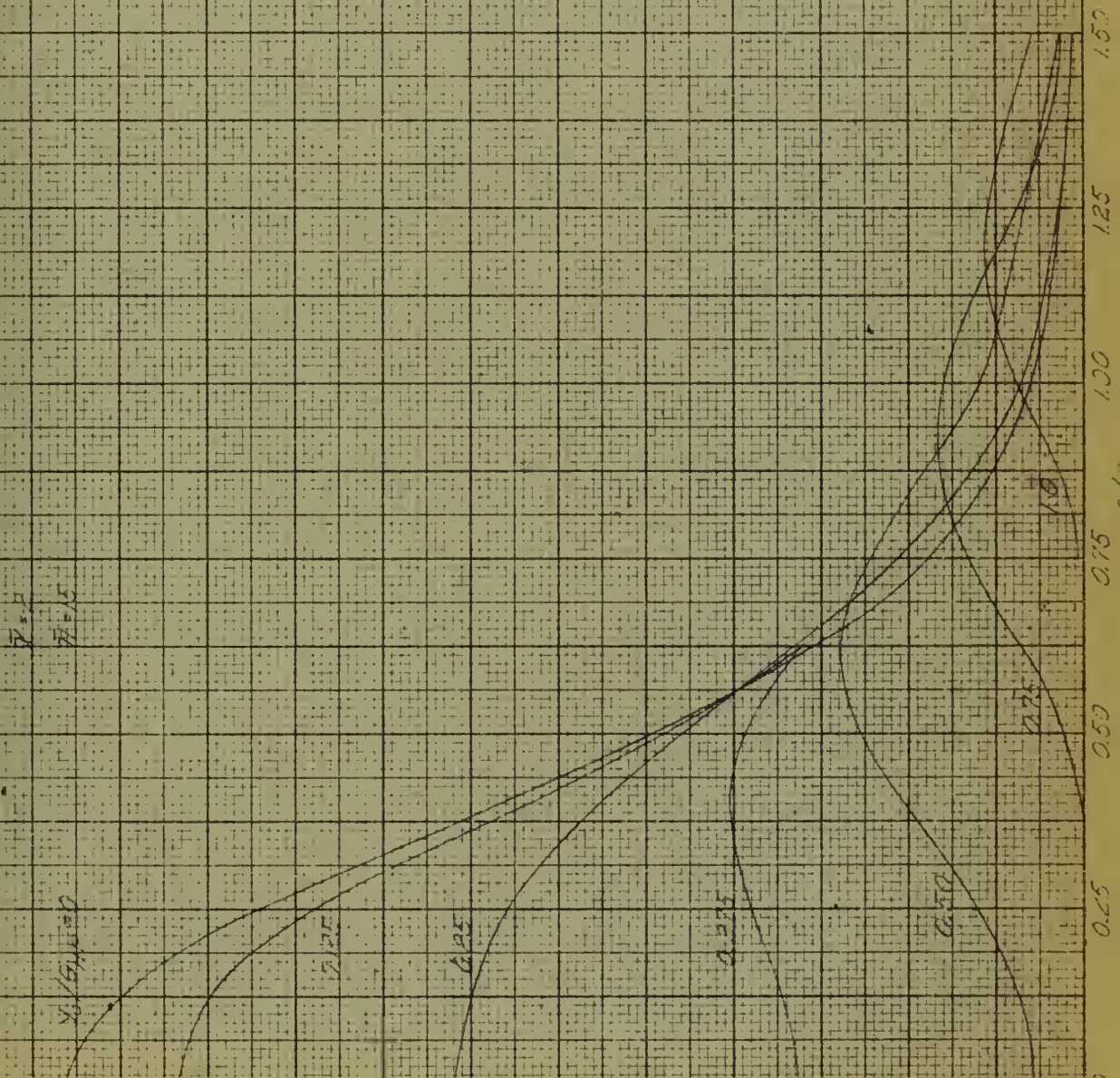
Effect of Varying Squint Angle

Figures 11 and 12 show the effect of changing the Squint angle in a Palmer Scan. It should be noted that as ρ is increased the elevation coverage is increased, but only at the expense of a decrease in the maximum probability of detection obtainable.

While, strictly speaking, the curves shown are applicable only for the values $\bar{n} = 15$ and $\bar{x} = 2$ they will retain the same general shape for moderate changes in these values.

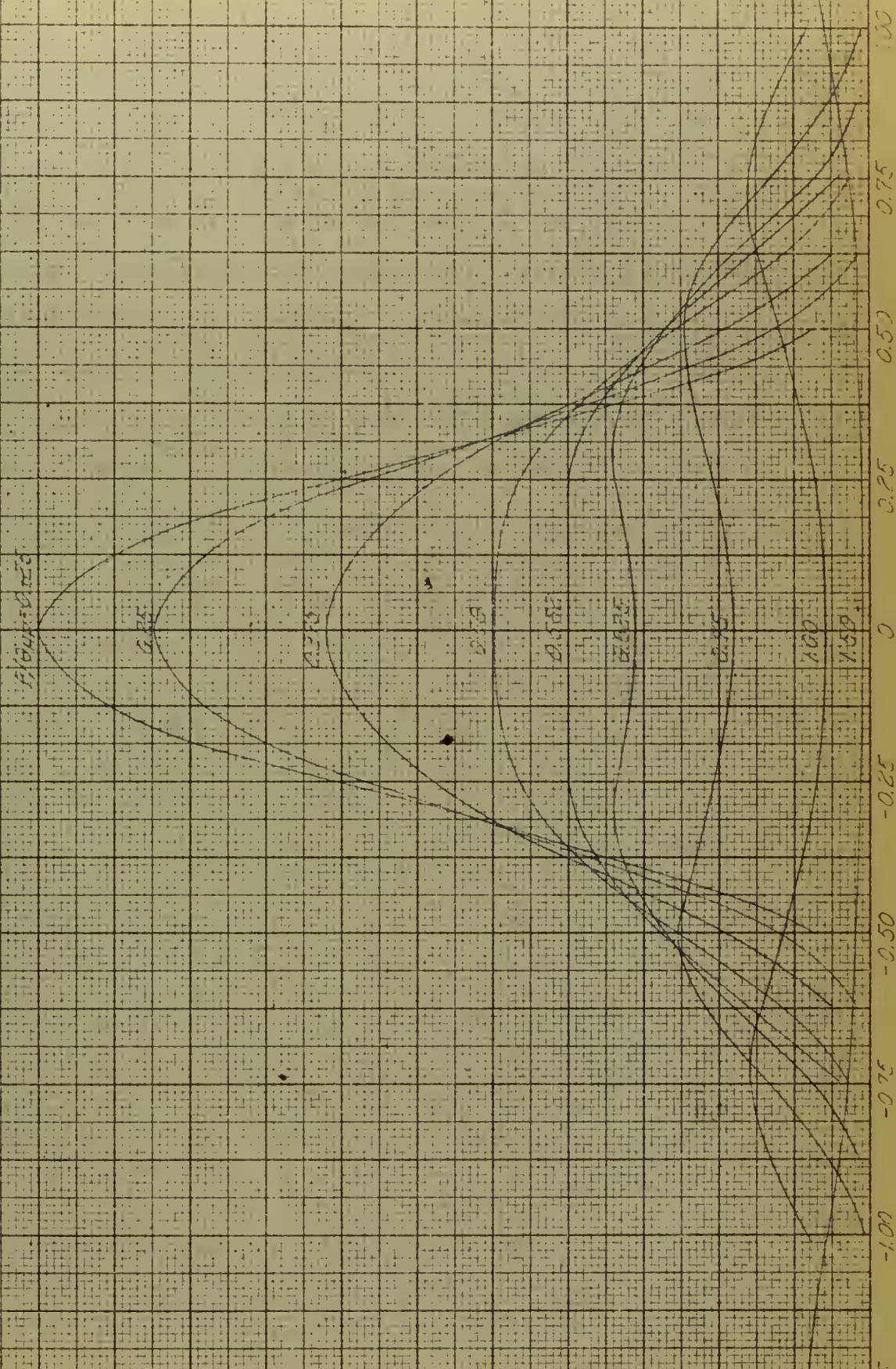
Palmer Scan, Variation of P_D
with Squint Angle for Various
Normalized Elevations

570: 11



Palmer Scan, Variation of P_D
with Normalized Elevation for
Various Squint Angles

Fig. 18



$P_D = 1$
 $\eta = 1.5$

Effect of Varying the Scan Frequency

In any Palmer Scan case where ρ , n and θ_{HP} are held constant, varying the scan frequency f will have no effect on the mean P_D . Caution must be exercised in the interpretation of this result for small integral values of PRF/f since the mean P_D represents a value averaged over initial phase. Once the scan has started the initial phase will remain fixed. Hence, for values of $PRF/f = 1, 2, 3$ or 4 , the Palmer Scan will degenerate into a line type scan. For values of $PRF/f > 5$ the variation of P_D with initial phase is of the same order as the variation with starting phase, which for the values of ρ , n , and θ_{HP} commonly used is reasonably small.

CHAPTER IV

CUMULATIVE PROBABILITY OF DETECTION

Thus far we have only considered the probability of detection for a single "look" at the target with a specified signal-to-noise ratio. In the actual use of the radar, where the antenna is continuously scanning and the range to the target is varying, we must consider the cumulative probability of detection, P_D^c

$$P_D^c = 1 - \prod_{i=1}^m (1 - P_D(i))$$

where $P_D(i)$ is the single look, or single cycle for multiple bar scans, probability of detection on the i^{th} look and m is the number of looks. The average signal-to-noise ratio at the beam center is related to the target R in the range equation $\bar{x} = k/R^4$. Taking R_0 as the range where $\bar{x} = 1$ $\bar{x} = (R/R_0)^{-4}$. Using the above relations one can plot curves showing the variation of single look P_D with normalized range R/R_0 for any scanning method. Figures 13 and 14 show the effect on single look P_D of changing range for a one bar linear scan and Figure 15 shows this effect for a two bar scanning cycle.

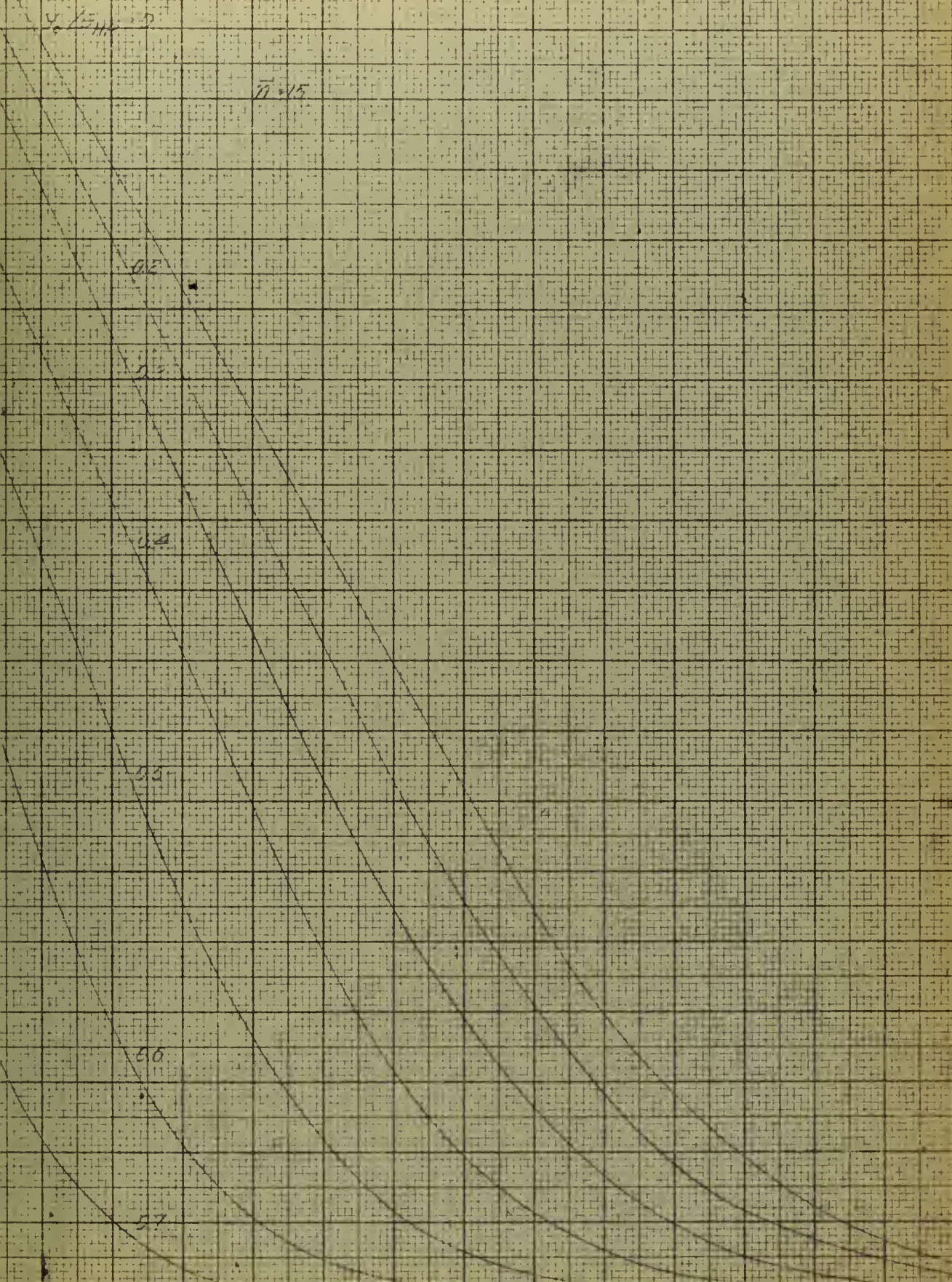
For most cases of practical importance the range to the target will be decreasing. Taking the normalized closing rate as $\Delta R/R_0$ per scan cycle, curves of P_D^c can be plotted. An example of the cumulative probability of detection is shown in Figure 16.

Linear Scan One Bar P_D as a
Function of R/R_0 for Various
Normalized Elevations

7-16-75

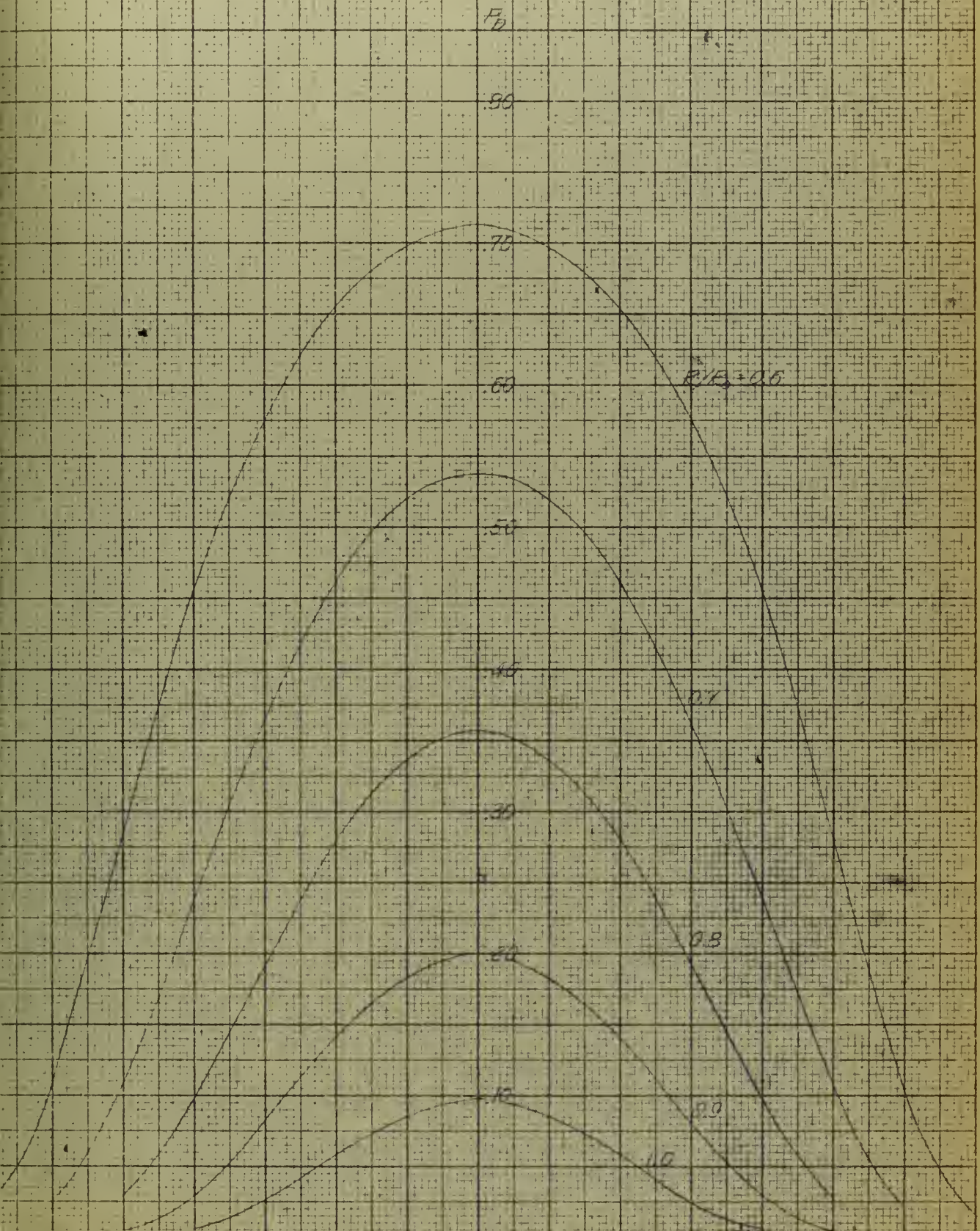
$Y_0/L = 0.111$

$\bar{H} = 15$



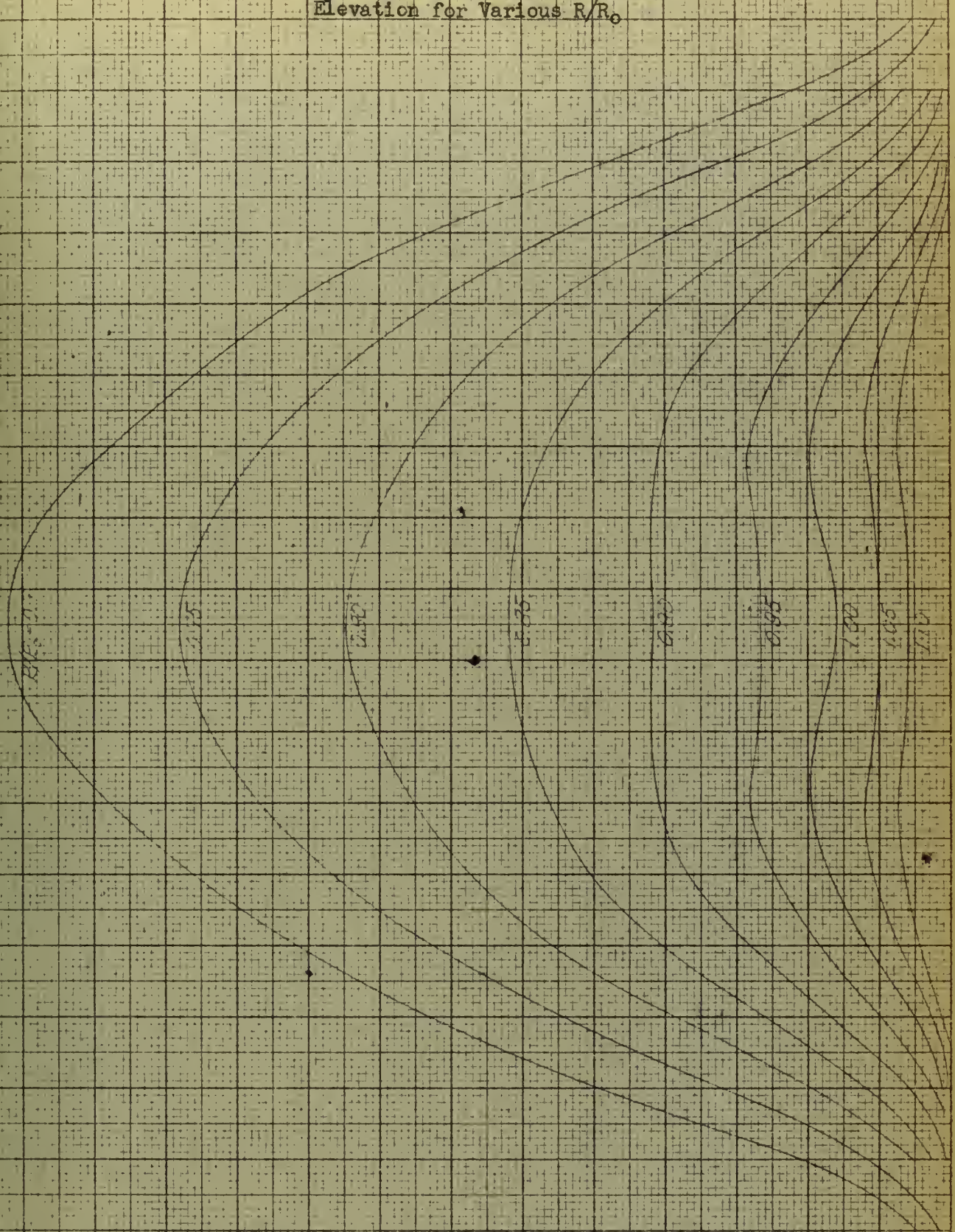
Linear Scan One Bar F_D as a
Function of Normalized Eleva-
tions for Various R/R_0

FIG. 14



Linear Scan, One Cycle Two Bar
 P_D as a Function of Normalized
 Elevation for Various R/R_0

FIG. 15



Linear Scan, One Bar Cumulative
Probability of Detection as a Func-
tion of R/R_0 for Various Normalized
Elevations.

FYB. 75

$R_0/E_{min} = 1.2$

$AP = 0.60$

2

3

$n = 15$

$AP = 0.559$

The desired result for any radar system is to detect the target at the longest possible range. To do this, when the target is located anywhere within a given area, we must scan the area so as to give a uniform maximum cumulative probability of detection throughout the area at any normalized range R/R_0 .

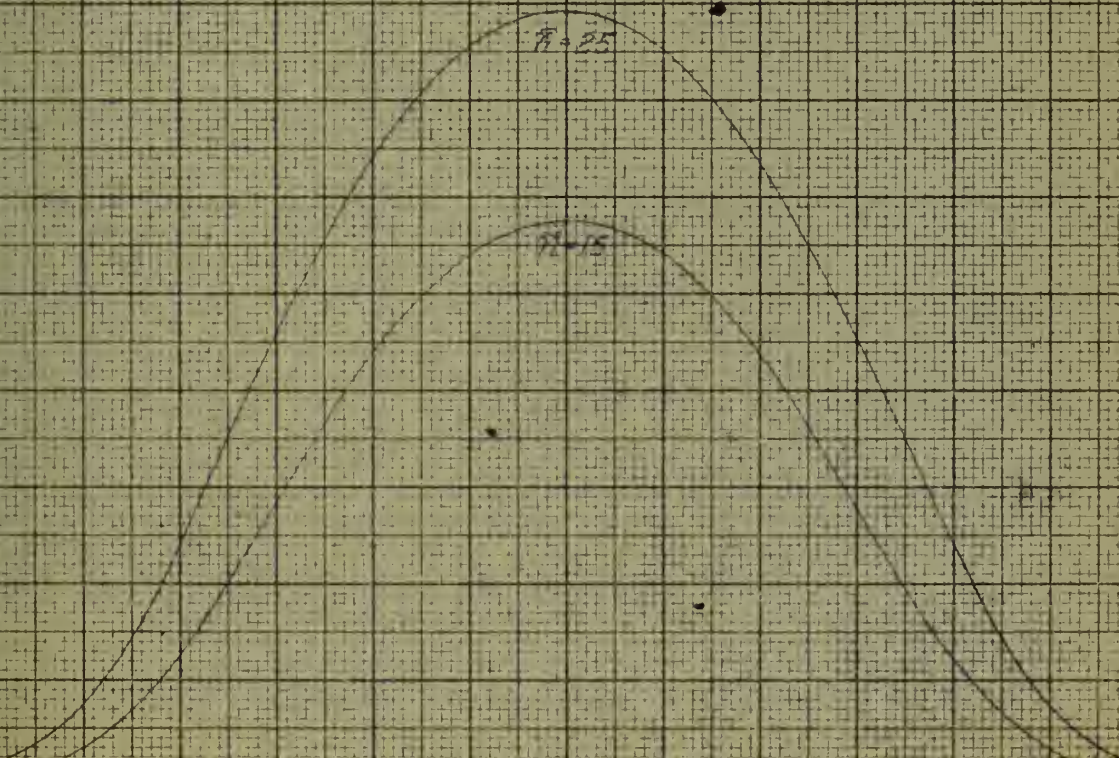
A scanning method which gives a higher single-look probability at a given range will give a higher cumulative probability if the area is scanned at the same rate. What is not quite so apparent is that the cumulative probability of detection for any given scanning method may, in many cases, be improved slightly by reducing the azimuth velocity and, therefore, increasing the time to complete a scan cycle. To illustrate this effect, consider the result of reducing v in a linear scan, with original scanning parameters such that $\bar{n} = 15$, to a new value $v' = 3/5 v$. The new number of pulses integrated, \bar{n}' , will be $\bar{n}' = 25$. Figure 17 shows the improved single look probability of detection at $\bar{x} = 2$. The cumulative probability of detection can be compared for the two velocities by using a value of $\Delta R'/R_0 = 5/3 \Delta R/R_0$, where $\Delta R'/R_0$ is the closing rate for the new velocity v' . Figures 18, 19 and 20 show the increase in P_D^C for closing rates of $\Delta R/R_0 = 0.01, 0.05$ and 0.10 respectively. It should be noted that the improvement is not very great and as the closing rate increases the improvement decreases which, for small R_0 and high closing rates, may detract from the desirability of decreasing v . In general we can say that a decrease in v which results in a

Linear Scan, One Bar Single
Look R_D for $n = 15$ and $n = 25$
as a Function of Normalized
Elevation

7-10-77

$n = 25$

$n = 15$



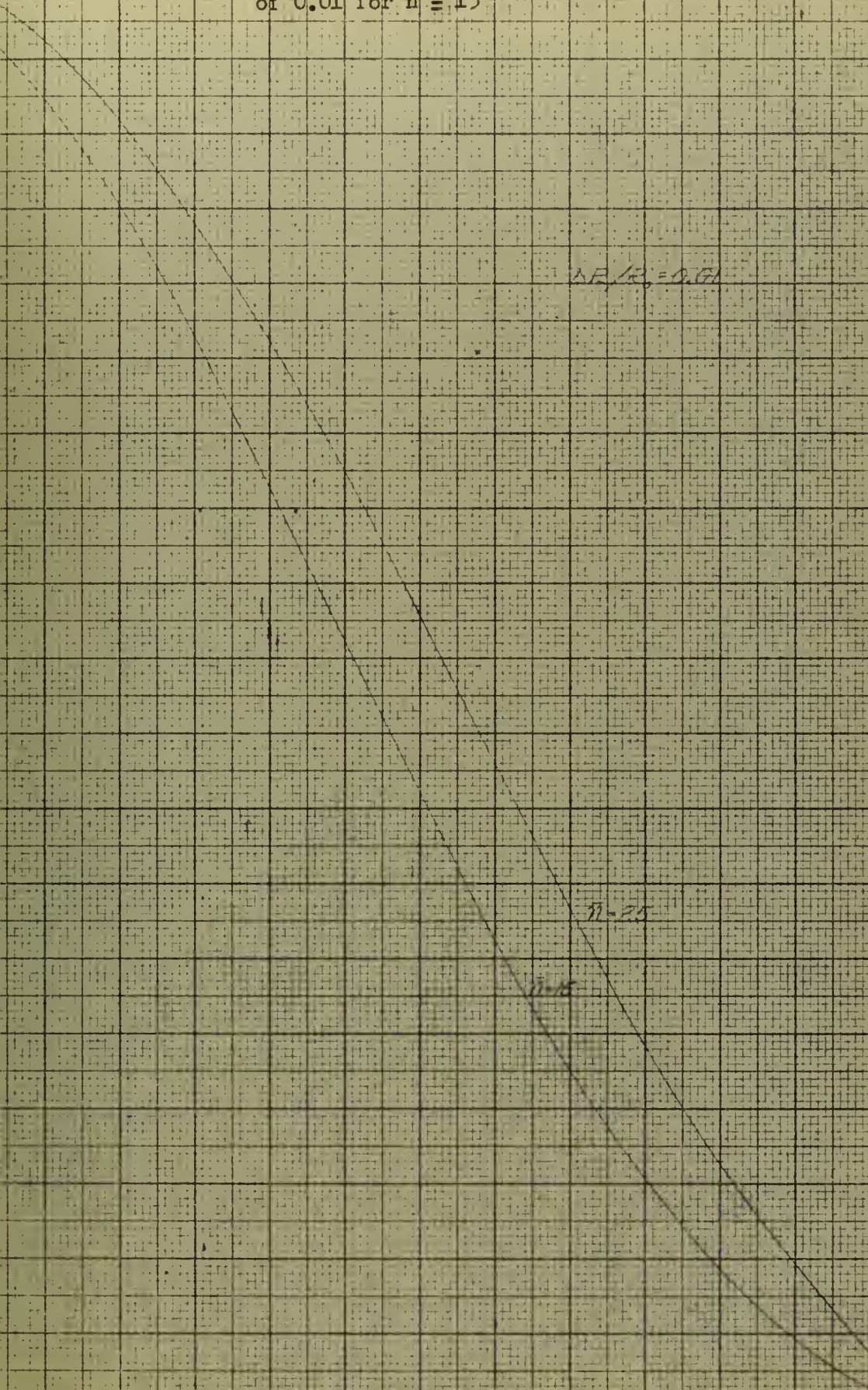
Linear Scan, One Bar Axial Cumulative
Probability of Detection as a Function
of R/R_0 for a Normalized Closing Rate
of 0.01 for $\bar{n} = 15$

FIG. 15

$\Delta R/R_0 = 0.01$

$\bar{n} = 25$

$\bar{n} = 15$



Linear Scan, One Bar Axial P_D vs R/R
for a Normalized Closing Rate of 0.05
for $\bar{n} = 15$

FIG. 10

$\Delta R/R = 0.05$

$\bar{n} = 25$

$\bar{n} = 15$

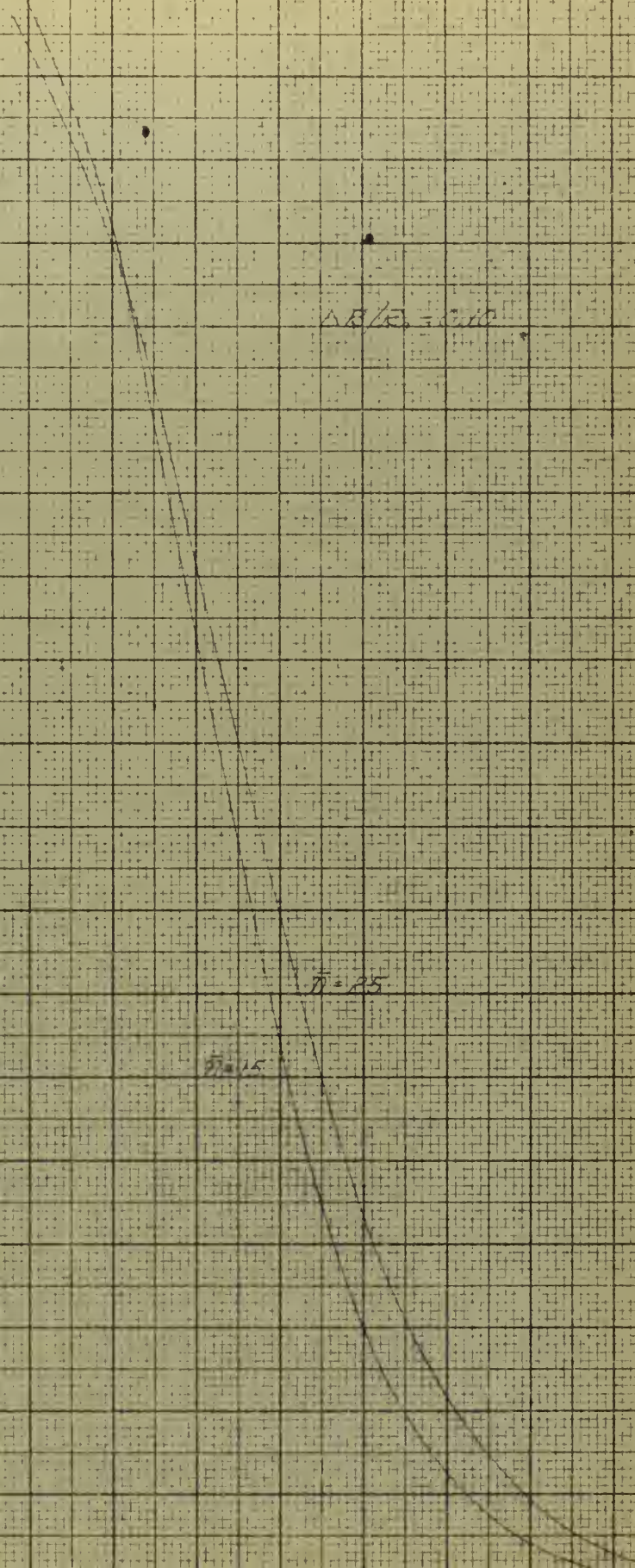
Linear Scan, One Bar Axial F_D vs R/R
for a Normalized Closing Rate of 0.10
for $n = 15$

FIG. 20

$\Delta R/R = 0.10$

$\bar{r} = 25$

$\bar{r} = 15$



significant increase in the single look P_D at a R/R_0 where \bar{x} is of the order of 1 or 2 will result in an increased cumulative probability of detection. A rough criterion for the increase is that a decrease in v of $B\%$ should be accompanied by an increase in P_D of $B\%$. Smaller increases in P_D must be investigated more closely for although they may give an increase in the lower values of P_D^C , the result of having a larger number of looks will be a larger P_D^C for the higher azimuth velocity as the range decreases.

Of the remaining parameters of a scanning system only the half power beam width and pulse repetition frequency can be varied to improve the cumulative probability of detection. The squint angle and bar spacing are determined by θ_{HP} if a uniform P_D^C is desired as shown in Figures 2, 3 and 12.

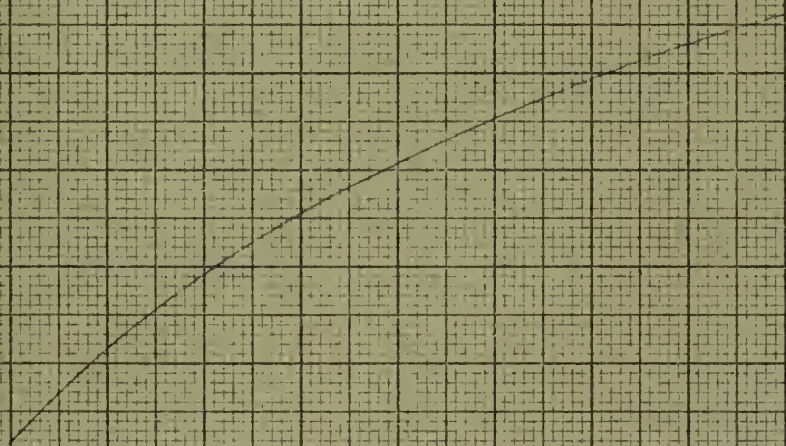
Figure 21 shows the normalized range, R/R_0 , at which $P_D^C = 0.85$ for a target closing at a normalized rate $\Delta R/R_0 = 0.05$ for a target on the axis of a one bar linear scan. A useful approximation, applicable to any type scan is that the normalized range at which $P_D^C = 0.85$ due to increasing the PRF to a new value k times the original PRF is:

$$(R/R_0)_{\text{new}}^{85} \approx k^{0.19} (R/R_0)_{\text{old}}^{85}$$

The improvement in the range at which $P_D^C = 0.85$ for $\Delta R/R_0 = 0.05$ achieved by reducing the half power beam width, with the system parameters readjusted to obtain a uniform single cycle probability of detection with the same azimuth velocity at low values of P_D , is shown in Figure 22. The azimuth velocity rather than the cycle time was maintained constant to keep the cumulative probability of detection from being decreased by an additional decrease in n due to

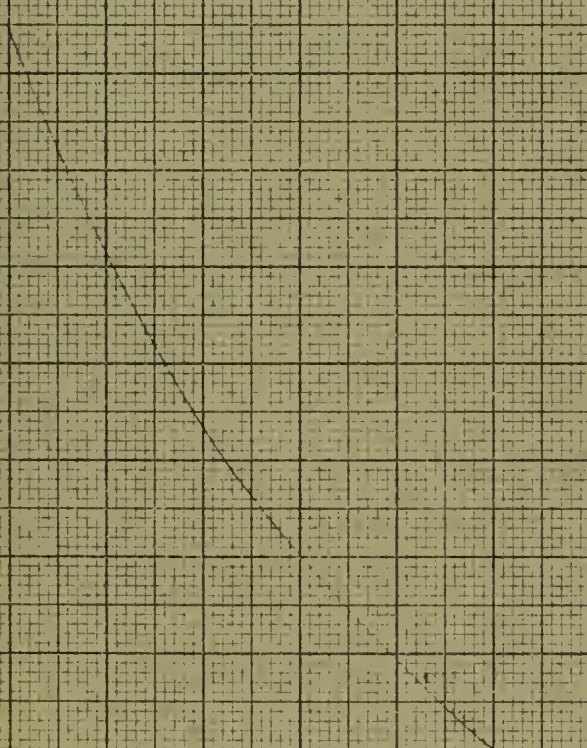
Normalized Range at Which F_D
= 0.85 as a Function of n

FIG. 21



Normalized Range at Which P_D
= 0.85 as a Function of Half
Power Beam Width

FIG 22



requiring that the area be covered in a given time and to keep the normalized closing rate constant.

Once again a rule of thumb to express the improvement can be stated. The improvement is approximately the ratio of the old θ_{HP} to the new raised to the 0.81 power. In terms of antenna diameters, D:

$$\text{Improvement} = \left(\frac{D_{\text{New}}}{D_{\text{Old}}} \right)^{0.81}$$

CHAPTER V

ILLUSTRATIVE EXAMPLE

As an example of the use of the information contained in the preceding chapters, let us consider a hypothetical case where it is required to scan an area 150° in azimuth and 7° in elevation. Normally the PRF and half power beam width are fixed by other design considerations; if not, Figures 21 and 22 show that the highest PRF and smallest half power beam width possible are the most desirable. For this example assume the PRF to be 400 pps and $\theta_{HP} = 4^\circ$. Figure 4 shows that a two bar Palmer Scan with a squint angle of 2° and bar separation of the 4° will give us the desired elevation coverage. As a starting point we can use an \bar{n} of 15. This corresponds to an azimuth velocity of slightly greater than $100^\circ/\text{sec}$ and a total time for a complete cycle of three seconds, including an allowance for the time required for the antenna to move between bars. Figure 23 shows the single look probability of detection for a two bar Palmer Scan with bars located at $y_0 = 0^\circ$ and 4° with $\bar{x} = 2$. Figure 4 also shows that a four bar linear scan will give us about a 7° elevation coverage. To keep the same cycle time, however, we must double our azimuth velocity reducing \bar{n} to 7.5. The single look P_D for this scan, with bars located at $y_0 = -1^\circ, 1^\circ, 3^\circ$ and 5° and $\bar{x} = 2$, is shown on Figure 23. By changing scanning methods we have achieved a 20% improvement in the center region and a greater improvement at the edges. As a final step let us decrease the azimuth velocity to give us a four second cycle,

$\bar{n} = 10$, and a six second cycle, $\bar{n} = 15$. The elevation coverage for these scans is also shown in Figure 23. To determine what, if any, improvement in the cumulative probability of detection has been achieved by changing the scanning methods we can examine P_D^C at a particular elevation. Figure 22 shows the cumulative probability of detection for a closing rate of 1200 knots and an R_0 of 20 miles at an elevation $y_0 = 0^\circ$. It can be seen that if we do not anticipate any closing rates much greater than 1200 knots, the six second cycle linear scan will have a value of $P_D^C = 0.85$ at the longest range.

It should be noted that the improvement gained in the value of R/R_0 for $P_D^C = 0.85$ by these changes is not very great, being about 3.5% for the change from the three second cycle Palmer Scan to the three second cycle linear scan with an additional 3.5% gain accruing from the change to a six second linear scan.

In the above example it was found that by using a two bar linear scan with twice the azimuth velocity the same area covered by a single bar of Palmer Scan could be scanned with about a 20% improvement in single look probability of detection. Further investigation disclosed that, with proper bar spacing, a two bar linear scan could be found which would cover the same elevation in the same time as a single bar of any of the methods employing vertical perturbations to increase elevation coverage and give an improvement in the single look probability of detection. By confining the comparison to schemes which give a reasonably flat P_D we essentially limit ourselves to cases of practical interest.

To illustrate why it will generally be better to scan an area in a given time with two bars of a linear scan, in preference to using one bar with vertical perturbations, let us consider these factors:

1. For the scans with vertical perturbations:
 - a. To have a constant P_D in elevation the value of $\sum_{i=1}^n a_i$ must be constant with elevation.
 - b. In any practical scanning method the pulses will be symmetrically distributed in elevation.
 - c. From Figure 1, in the region $.05 < P_D < .50$, to maintain P_D constant when doubling n , $\bar{x} \sum a_i$ must be multiplied by a factor of 1.25.
 - d. The elevation over which we can achieve a flat P_D without too great a sacrifice in the maximum value of P_D is limited to about $0.75 \theta_{HP}$, as shown in Figures 2 and 12.
2. In Figure 15 we see that for the linear scan case, with a bar separation of $0.5 \theta_{HP}$, P_D will be reasonably constant between bars in the region $\bar{x} \approx 2$, which is the region in which P_D^c reaches values greater than 0.50, and give an elevation coverage of about $0.75 \theta_{HP}$.
 - a. If the two bar linear scan has a higher single cycle probability of detection at the extremities of the region of elevation it will have a greater probability over the whole region.
3. For a given number of pulses the maximum average value of $\sum_{i=1}^n a_i$ is achieved when the beam center positions are all at the same elevation and the target is also at this elevation.

From the last item and l.b. it can be seen that the scanning system employing vertical perturbations which will give the largest constant value for $\sum_{i=1}^n a_i$ over a given elevation is the two line scan. Since this value will be at the elevation of a line of pulses and will therefore be greater than that for a scheme in which the pulses are not arranged in a line. For a two line scan a squint angle of $0.35 \theta_{HP}$ will give practically a constant value for the summation for elevations between $\pm \rho$. At an elevation equal to the squint angle the value of the summation is:

$$a_i = 1.07 \frac{n}{2} A.$$

where $A =$ the value of $\frac{2}{n} \sum_{i=1}^n a_i$

However, for a two bar linear scan with bars at $0.25 \theta_{HP}$ above and below the original scan axis and having twice the azimuth velocity as the previously considered two line scan the value of the summation, for which the number of pulses integrated is $n/2$, will be:

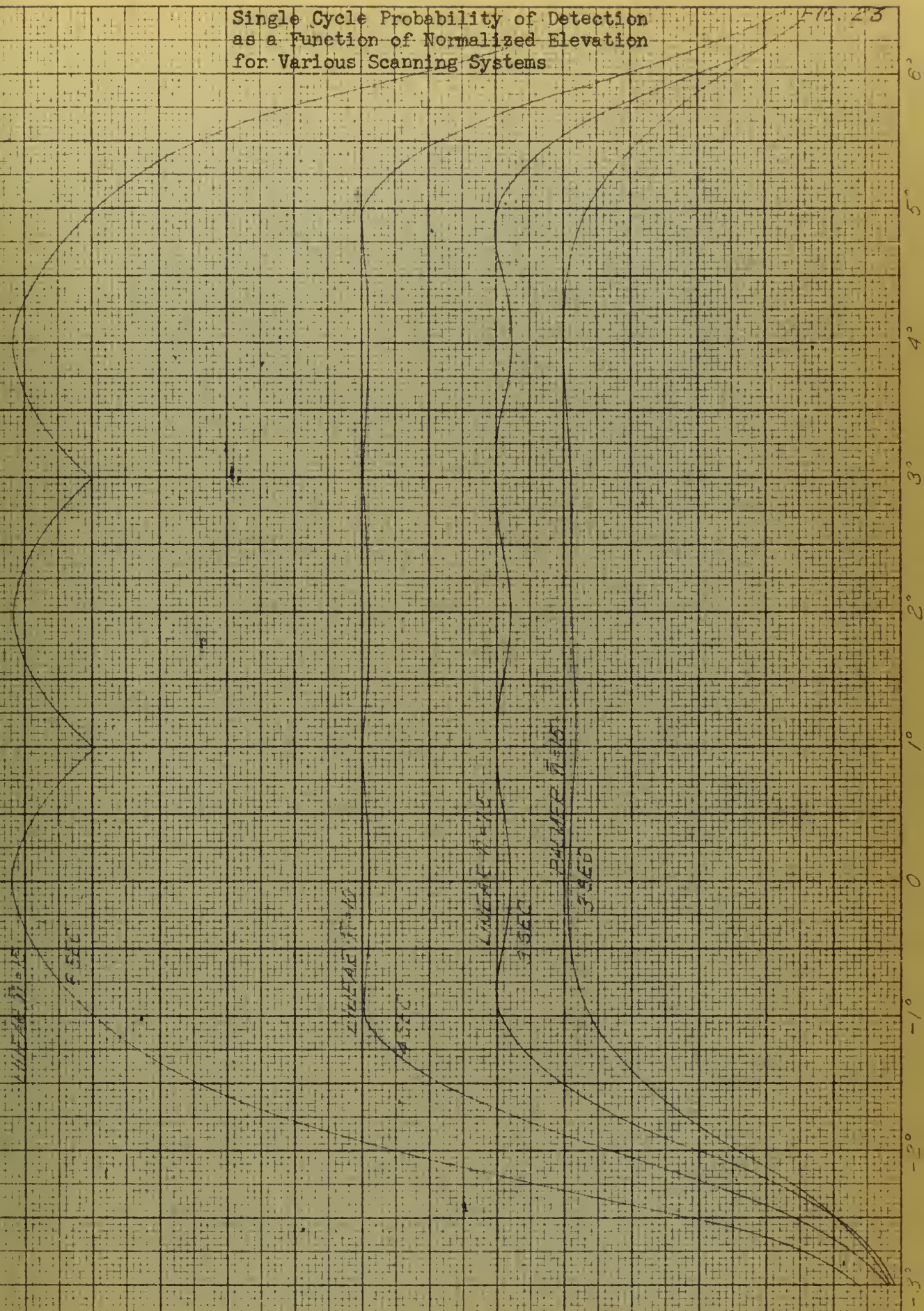
$$a_i = 0.946 \frac{n}{2} A$$

which is greater than $1/1.25 \sum_{i=1}^n a_i$ (sec 1 (c)).

Hence, the single cycle probability will be greater at this point than for the two line scan.

Single Cycle Probability of Detection
as a Function of Normalized Elevation
for Various Scanning Systems

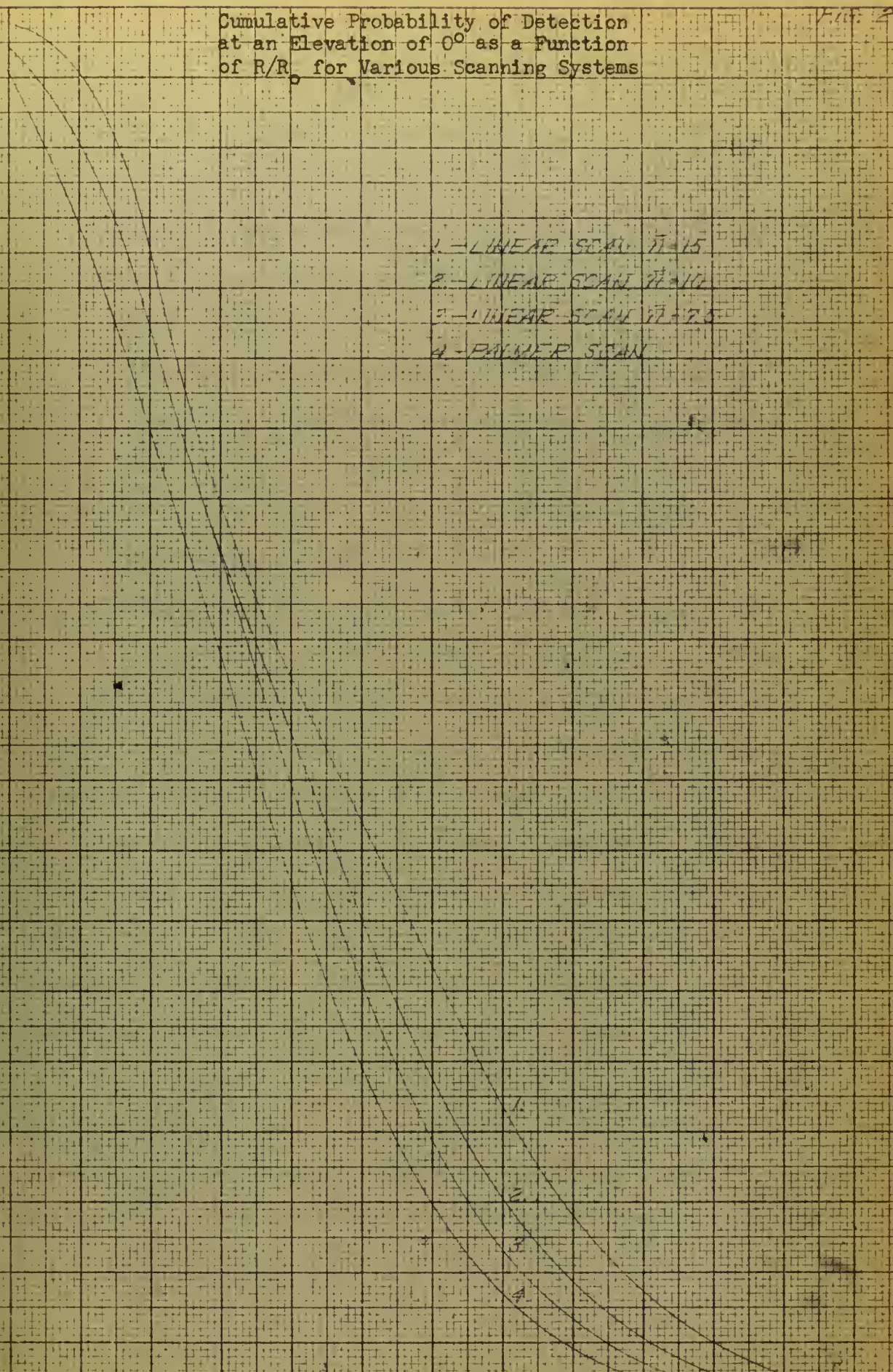
Fig. 23



Cumulative Probability of Detection
at an Elevation of 0° as a Function
of R/R_0 for Various Scanning Systems

Fig. 24

- 1 - LINEAR SCAN $\eta = 15$
- 2 - LINEAR SCAN $\eta = 10$
- 3 - LINEAR SCAN $\eta = 7.5$
- 4 - PALMER SCAN



CHAPTER VI

DISCUSSION OF RESULTS

In the preceding chapters it has been shown that the most effective coverage of a given area by a scanning radar is obtained when the scan system parameters are:

1. The pulse repetition frequency is as high as possible consistent with maximum peak power for the transmitter.
2. The half power beam width is as small as possible.
3. The scan used is a linear scan with bar separation of one-half the half power beam width.
4. The azimuth velocity is adjusted to give a P_D^C of 0.85-0.9 at the longest range for a given maximum closing rate.

The slight advantage gained from using a linear scan may be outweighed, in a fire control radar, by the increased mechanical complexity required to provide this scan and a tracking mode. If the Palmer Scan is desired, on the basis of expediency, the system should have a squint angle of one-half the half power beam width and a bar separation equal to the half power beam width. The squint angle represents a compromise between elevation coverage and single look probability of detection and may be varied somewhat. (See Figure 12)

The bar spacing, however, represents a value which will give a uniform elevation coverage. The extremely rapid decrease in the probability of detection at elevations greater than the squint angle, see Figure 2, makes the bar separation very critical if one does not

desire to have holes in the detection pattern. As an additional item it should be pointed out that the commonly used rule that antenna coverage can be considered to extend out to the half power points is seriously in error. For example Figure 2 shows that, at the half power point, $y_0 = 0.5 \theta_{HP}$, the single look P_D for a linear scan is only 6% of the value on the axis.

BIBLIOGRAPHY

1. Campbell, G. A. and Foster, R. M. FOURIER INTEGRALS FOR PRACTICAL APPLICATIONS, D. Van Nostrand Co., 1947: Also Bell Telephone System Monograph No. B-584
2. Drukey, D. L. RADAR RANGE PERFORMANCE, Hughes Aircraft Company Technical Memorandum No. 277, 15 April 1947
3. Lawson, J. L. and Uhlenbeck, G. E. THRESHOLD SIGNALS, Vol. 24 of MIT Radiation Laboratory Series, McGraw-Hill, 1948
4. Marcum, J. I. A STATISTICAL THEORY OF TARGET DETECTION BY PULSED RADAR - MATHEMATICAL APPENDIX, Rand Research Memorandum RM-753, 1 July 1948
5. Marcum, J. I. A STATISTICAL THEORY OF TARGET DETECTION BY PULSED RADAR, Rand Research Memorandum RM-754, 1 December 1947
6. Middleton, D. SOME GENERAL RESULTS IN THE THEORY OF NOISE THROUGH NONLINEAR DEVICES, Quarterly of Applied Mathematics, Vol. 5, January 1948
7. Pearson, K. TABLES OF THE INCOMPLETE GAMMA FUNCTION, Biometrika Office, University College, London, 1934
8. Rice, S. O. THE MATHEMATICAL ANALYSIS OF RANDOM NOISE, Bell System Technical Journal, Vol. 23, pp 282 - 332, July 1944 and Vol. 24, pp 45 - 156, January 1945
9. Ridenour, L. N. RADAR SYSTEMS ENGINEERING, Vol. 1 of MIT Radiation Laboratory Series, McGraw-Hill, 1947
10. Swerling, P. PROBABILITY OF DETECTION FOR FLUCTUATING TARGETS, Rand Research Memorandum RM-1217, 17 March 1954

APPENDIX I

DERIVATION OF EXPRESSION FOR PROBABILITY OF DETECTION

The probability density of the envelope, R , of a sinusoidal signal plus Gaussian noise, S , which has been passed through a narrow band filter, $S = A \cos \omega t + N(t)$, has been shown by Rice⁸ and others to have

$$\begin{aligned} \text{the form, } f(R, A) &= \frac{R}{\psi_0} e^{-\left(\frac{R^2 + A^2}{2\psi_0}\right)} I_0\left(\frac{RA}{\psi_0}\right), \quad R \geq 0 \\ &= 0, \quad R < 0 \end{aligned}$$

where ψ_0 is the average noise power at the output of the receiver and $I_0(x)$ is the Bessel function of imaginary argument. The effect of passing the signal through a square law detector can be analyzed by introducing a pair of dimensionless variables

$$x = \frac{A^2}{2\psi_0}$$

$$y = \frac{R^2}{2\psi_0}$$

The probability that an observed value of the normalized output of a square detector will lie between y and $y+dy$ can be written as

$$f(x, y) dy = e^{-x-y} I_0(2\sqrt{xy}) dy$$

The characteristic function is by definition the Fourier transform of a given probability density function

$$C(p, x) = \int_0^\infty f(x, y) e^{py} dy; \quad p = j\omega$$

For a single pulse

$$C_1(p, x) = \int_0^\infty e^{-x-y} e^{py} I_0(2\sqrt{xy}) dy$$

Using pair 655.5 of the Campbell Foster tables¹

$$C_1(p, x) = 1/p+1 \quad e^{-x(p/p+1)}$$

If the signal-to-noise ratio were constant for the n pulses in a scan, which would be the case for an antenna with constant gain and a slowly scintillating target for which the return is constant over a scan but varies independently from scan to scan, the characteristic function for the sum of n pulses would be

$$C_n(\rho, x) = \frac{1}{(\rho+1)^n} e^{-nx(\frac{\rho}{\rho+1})}$$

However, in the actual case the signal-to-noise ratio for a target not on the antenna beam axis will be reduced. From the radar range equation⁹

$$x_i = \frac{PG^2 \sigma F \lambda^2}{(4\pi)^3 R^4 k T B \overline{NF}}$$

where

x_i = Actual signal-to-noise ratio

P = Peak transmitted power, in watts

G = Actual antenna gain in the target direction

σ = The target cross section

F = Factor which allows for plumbing and other losses on both transmission and reception

R = Range to target

B = Band width in cps

\overline{NF} = Receiver noise figure

T = Absolute temperature

k = Boltzman's constant, 1.38×10^{-23} joules/degree.

The signal-to-noise ratio for the i^{th} pulse can be written as $x_i = a_i x$

where

x = The signal-to-noise ratio for a target on the beam axis

$$a_i = G_i^2 / G_o^2$$

G_o = The antenna gain on the beam axis

Taking the antenna gain into consideration

$$C_n(p, x) = 1/(p+1)^n e^{-x \sum_{i=1}^p a_i} (p/p+1)$$

For a slowly scintillating target consisting of a large number of independent scatterers of the same order of magnitude, the probability density of the signal-to-noise ratio is given by

$$P(x) = 1/\bar{x} e^{-x/\bar{x}}, x \geq 0$$

where

\bar{x} = The average signal-to-noise ratio over all target fluctuations for a target on the beam axis.

Middleton⁶ has shown that it is permissible to average over all phases. Therefore, the average characteristic function will be given by

$$\begin{aligned} \overline{C_n(p, x)} &= \int_0^\infty P(x) C_n(p, x) dx \\ &= \frac{1}{\bar{x}(p+1)^n} \int_0^\infty e^{-x/2(1 + \frac{A}{p+1})} dx \\ &= \frac{1}{(p+1)^{n-1} [1 + p(1+A)]} \end{aligned}$$

where

$$A = \bar{x} \sum_{i=1}^p a_i$$

The density function $f(x, y)$ is, from pair 580.7 of the Campbell Foster tables¹,

$$\begin{aligned} f(x, y) &= \frac{1}{1+A} \cdot \frac{1}{\Gamma(n-1)(1 - \frac{1}{1+A})} e^{-\frac{y}{1+A}} \\ &\quad \times \gamma[(n-1), (1 - \frac{1}{1+A})y] \\ &= (1 + \frac{1}{A})^{n-2} \frac{1}{A} \left\{ 1 - \frac{\Gamma(n-1, \frac{y}{1+A})}{\Gamma(n-1)} \right\} e^{-\frac{y}{1+A}} \end{aligned}$$

where $\delta[v, z] = \Gamma(v) - \Gamma(v, z)$

Using the notation of Pearson⁷

$$1 - \frac{\Gamma[(n-1), \frac{y}{1+A}]}{\Gamma(n-1)} = I\left(\frac{y}{(1+A)\sqrt{n-1}}, n-2\right)$$

$$f(x, y) = (1+A)^{n-2} \frac{1}{A} I\left(\frac{y}{(1+A)\sqrt{n-1}}, n-2\right) e^{-\frac{y}{1+A}}$$

The criterion for detection is that when the sum of the n outputs from the detector exceeds a certain bias level, say Y_D , the operator will decide that a target is present.

The bias level is chosen to yield a suitable false alarm probability P_{FA} which is the probability that noise alone will exceed the bias level during the time of one decision.

In this case:

$$x = 0$$

$$C_1(p, 0) = \frac{1}{p+1}$$

$$C_n(p, 0) = \frac{1}{(p+1)^n}$$

$$f(0, y) = \int_{-\infty}^{\infty} \frac{1}{(p+1)^n} e^{-py} \frac{dy}{2\pi}$$

$$P_{FA} = \frac{1}{(n-1)!} \int_0^{\infty} y^{n-1} e^{-y} dy$$

The probability of detection P_D is

$$P_D = 1 - \int_0^{Y_D} f(x, y) dy$$

Swerling¹⁰ has shown a simple means of evaluating the above expression

by considering $\overline{C_n(p, x)} = \frac{1}{(p+1)^{n-1}}$

$$\overline{C_n(p, x)} = \frac{1}{(p+1)^{n-1}} = -p(1+A) \overline{C_n(p, x)}$$

$$\overline{C_n(p, x)} = \frac{1}{(p+1)^{n-1} - p(1+A) \overline{C_n(p, x)}}$$

$$f(x, y) = \frac{y^{n-2} e^{-y}}{(n-2)!} - (1+A) f'(x, y)$$

$$\int_0^{y_0} f(x, y) dy = \int_0^{y_0} \frac{y^{n-2} e^{-y}}{(n-2)!} dy - (1+A) f(x, y_0)$$

$$P_0 = 1 - I\left[\frac{y_0}{\sqrt{n-1}}, n-2\right] + (1+A)^{n-1} e^{-\frac{y_0}{1+A}} I\left[\frac{y_0}{(1+A)\sqrt{n-1}}, n-2\right]$$

Consideration of Pearson's tables⁷ shows that

$$I\left[\frac{y_0}{(1+A)\sqrt{n-1}}, n-2\right] > I\left[\frac{y_0}{\sqrt{n-1}}, n-2\right], \quad I[a, b] \leq 1$$

and that $I\left[\frac{y_0}{\sqrt{n-1}}, n-2\right]$ decreases with increasing n , for a given P_{FA} . For the cases considered in this paper $P_{FA} = 10^{-6}$ and $n = 49$. For the values $n = 49$, $P_{FA} = 10^{-6}$, $I\left[\frac{y_0}{\sqrt{n-1}}, n-2\right] = 0.999994$.

The above values will give the largest error in the approximate expression

$$P_D = (1 + 1/A)^{n-1} e^{-\frac{y_0}{1+A}}$$

For values of $P_D = 0.001$, the error resulting from using the approximation will be less than 0.4%.

APPENDIX II

DESCRIPTION OF APPROXIMATE METHOD FOR OBTAINING PROBABILITY OF DETECTION

Initial computations of the probability of detection for a number of cases using point by point calculations with $n \approx 15$ and $\rho \approx \frac{1}{2} \theta_{HP}$ disclosed that the variation of P_D with azimuth for a fixed elevation was surprisingly small, being no greater than $\pm 10\%$ of the mean. This lead to the following scheme for determining an approximate P_D as a function of elevation:

In the expression

$$\sum_{i=1}^n a_i = \sum_{i=1}^n e^{-\frac{2}{\theta^2}(x_0 - x_i)^2} e^{-\frac{2}{\theta^2}(y_0 - y_i)^2}$$

where (x_0, y_0) is the position of the target and (x_i, y_i) is the i^{th} position of the beam center replace $e^{-2/\theta^2(x_0 - x_i)^2}$ by the average azimuth contribution for a corridor width W centered at $x_0 = 0$

$$\frac{1}{W} \int_{-\frac{W}{2}}^{\frac{W}{2}} e^{-x^2} dx = \left(\frac{\sqrt{\pi}}{W} \frac{\theta_0}{\sqrt{2}} \right) \text{erf} \left(\frac{W}{\sqrt{2} \theta_0} \right)$$

and let $f(y_{j1} \bar{n})$ be the average number of pulses at an elevation y_j .

$$a \bar{n} = \left(\frac{\sqrt{\pi}}{W} \frac{\theta_0}{\sqrt{2}} \right) \text{erf} \left(\frac{W}{\sqrt{2} \theta_0} \right) \sum_{j=1}^m f(y_j, \bar{n}) e^{-\frac{2}{\theta^2}(y_0 - y_j)^2}$$

$$P_D \approx \left(1 + \frac{1}{\bar{n} a} \right)^{n-1} e^{-\frac{y_0^2(\bar{n})}{1 + \bar{n} a}}$$

$$\bar{n} = W \frac{PRF}{V}$$

Using $f(y_j, \bar{n}) = \bar{n}$ - linear scan

= $0.5\bar{n}$ - at each elevation, y_j , of the two line scan

= $0.333\bar{n}$ - at each y_j for the three line scan

$$= \frac{\bar{n}}{\pi} \int_{y_1-4y}^{y_1+4y} \frac{1}{\sqrt{1-(y/\rho)^2}} dy \quad \text{for the Palmer Scan}$$

the results obtained by the above approximation were compared with the value of P_D averaged over both starting phase and initial phase, where applicable. The agreement was remarkably good. In the line scan cases the error was only a few percent, less than 5%, for cases in which the number of pulses on a line was less than four with the larger errors for small number of pulses on a line. For the Palmer Scan the error was found to increase with the squint angle as well as for decreasing \bar{n} , being $\pm 15\%$ for the extreme case considered in which $\rho = 1.5 \theta_{HP}$ and $\bar{n} = 10$ with the value of P_D on the axis of $P_D \approx 0.10$.

In all cases considered the value obtained by use of this approximation was of the order of the exact mean $P_D \pm 0.01$ except for values of P_D less than 0.07 where it was of the order of the exact mean $P_D \pm 0.007$ and in all cases was less than the maximum deviation of the actual case from the mean.

LE 2856

INTERLIB

Naval Research Lib

11 Mar'64 INTERLIBRARY LOAN
(Hughes Aircraft,
Culver City)

7 Aug'64 INTERLIBRARY LOAN

The is
P362

Perszyk

The effects of
scanning on the detect-
ion of targets.

28469

LE 2856

INTERLIB

Naval Research Lib

11 Mar'64 INTERLIBRARY LOAN
(Hughes Aircraft,
Culver City)

7 Aug'64 INTERLIBRARY LOAN
[Hughes aircraft
Culver City]

20 Jul'65 INTERLIBRARY LOAN

28469

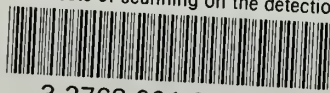
Thesis
P362

Perszyk

The effects of scanning on
the detection of targets.

thesP362

The effects of scanning on the detection



3 2768 001 98004 8

DUDLEY KNOX LIBRARY